Journal of The Electrochemical Society

Review—Reversible Heat Effects in Cells Relevant for Lithium-Ion Batteries

Journal of The Electrochemical Society, 2021 **168** 050522

Review—Reversible Heat Effects in Cells Relevant for Lithium-Ion Batteries

Astrid F. Gunnarshaug,[1] Preben J. S. Vie,[2,3] and Signe Kjelstrup[1,z]

[1]*PoreLab, Department of Chemistry, Norwegian University of Science and Technology, NTNU, Trondheim, Norway*
[2]*Institute for Energy Technology, Kjeller, Norway*
[3]*Department of Energy and Process Technology, Norwegian University of Science and Technology, NTNU, Trondheim, Norway*

We review measurements of reversible heat effects in lithium-ion batteries, i.e. entropy changes and Seebeck coefficients of cells with relevant electrodes. We show how to compute the Peltier heat of battery electrodes from Seebeck coefficients. The Seebeck coefficient depends on the heat of transfer (Soret effect), which is found from the difference of initial and stationary state values of the Seebeck coefficient. We apply non-equilibrium thermodynamics theory and obtain initial Peltier heats not reported before. For the oxidation of lithium metal we propose the value 34 ± 2 kJ mol^{-1} when the electrolyte contains 1 M $LiPF_6$, while the value is 29 ± 1 kJ mol^{-1} when the electrolyte contains 1 M $LiClO_4$. The positive values imply that the electrode cools when it serves as an anode. For oxidation of lithium under stationary state conditions, the stationary state Peltier heat is $\approx$120 kJ mol^{-1}. A large reversible heating effect can then be expected for the single electrode; much larger than expected from the full-cell entropy change. These values have a bearing on thermal modelling of batteries. Peltier heats for anodic reactions are presented in tables available for such modelling. We discuss the need for measurements and point at opportunities.
 [DOI: 10.1149/1945-7111/abfd73]

Manuscript submitted March 3, 2021; revised manuscript received April 9, 2021. Published May 13, 2021.

Lithium-ion batteries (LIB) have become among the world's leading battery technology when it comes to energy storage.[1] The electrodes of the LIB contain lithium in intercalated form, while the electrolyte consists typically of two or more organic components (the solvent) and one lithium salt.[2] LIB-applications have evolved from the use of single batteries in small hand-held devices to large battery packs in electrified vehicles,[3] even boats and ferries.[4] The new applications have added new demands on life-time expectancy, capacity and safety.

It is well know that the temperature plays a role in the LIB's performance. Thermal- and degradation modelling has therefore been a topic of interest for decades.[5–7] Accurate thermal models may for instance help us understand and control the ageing mechanisms.[8,9] The accuracy of single-cell thermal modelling is rather important for modelling of larger battery packs.[9–11]

Among the thermal effects in LIB, *i.e.* Joule heating, heating due to electrode overpotentials and reversible heat effects, the reversible ones are special in their relation to the cell entropy changes. The entropy change of an electrochemical cell follows from the electrode reactions and the charge transfer in the electrolyte. It is customary in the battery literature to speak of a complete battery as a full-cell, while a so-called half-cell contains one battery electrode and one lithium metal electrode. The two cells are illustrated schematically in Figs. 1 and 2. We shall adopt this terminology for the convenience of the battery community. A lithium cobalt oxide, $LiCoO_2$ (LCO), half-cell will then contain one LCO electrode and one Li metal electrode, see Fig. 2. We discuss both full- as well as half-cells in this review. It was often discussed in the literature,[12] that reversible heat effects can be neglected when compared to irreversible effects in thermal models, at least at medium and high charge/discharge rates.[13] Lately there is, however, an emerging agreement that reversible heat effects need be included in all thermal modelling.[14,15] But this has most often been done for LIBs by including the total reversible heat effect of the cell, or the entropy change of the cell reaction. The total effect has been evenly distributed over the cell. However, since the electrodes are positioned at separate locations in a unit cell, the local heat effect at one electrode surface, may differ from the average total effect. While the local effects always sum to the total one, they need not be equal fractions of the total everywhere. Each local effect can be larger or smaller than the total effect, and they can even have different signs. Local cooling effects are not only possible. They have been observed.[16,17] By looking at the local reversible effects from the perspective of non-equilibrium thermodynamics, we shall see here that they indeed are significantly larger than the total reversible effects in LIB cells. An important message will emerge: Reversible heat effects could play a more important role in battery modelling at high charge/discharge rates than believed so far.

There is much confusion in the literature on the relation between the entropy change of the lithium half-cell and the entropy change at the lithium electrode. The first quantity is measured, according to classical thermodynamics, as the temperature dependence of the *emf*, cf. Eq. 1. When this coefficient is multiplied with the temperature, it expresses the total reversible heat taken from the surroundings and used in the cell. An error arises if this quantity is interpreted as the reversible heat change of one electrode only.[6,17,18] In this interpretation, an assumption is made, that the local reversible heat effect around the lithium metal counter electrode, or the Peltier heat of this electrode surface, is zero. This is not the case, as we shall see later in the article. The Peltier heat for Li metal is in fact rather large. To localize the reversible heat effect of a half-cell to one of the electrodes only, will in turn produce models with incorrect local temperature gradients, and potentially mask battery health problems. One motivation for the present review has been a wish to clarify these issues. In order to do so and we shall re-evaluate reported results from the theoretical perspective given by non-equilibrium thermodynamics.[19,20]

According to this theory, the Peltier heat can best be determined by measuring its reciprocal effect, the Seebeck coefficient. There are reports in literature on the Seebeck coefficient of cells with Li metal electrodes. These indicate that the Peltier heats are large.[18,21,22] A few reports of Seebeck coefficients can be found for cells with electrodes of materials relevant to the LIB.[16,18,21–24] The primary motivation for these experiments were their relevance to thermo-galvanic cells, however, and the purpose of that research was to contribute to waste heat energy harvesting. This is an interesting application, but the results obtained are equally useful for LIBs! This appears to have gone largely unnoticed. A purpose of this review is therefore to review thermoelectric cells that can give information on reversible heat effects in LiB.

The Peltier heat has usually not been included in LIB thermal models. Many authors have proposed to do so,[5] but as far as we know, the first report on the topic was only recently presented.[11]

[z]E-mail: signe.kjelstrup@ntnu.no

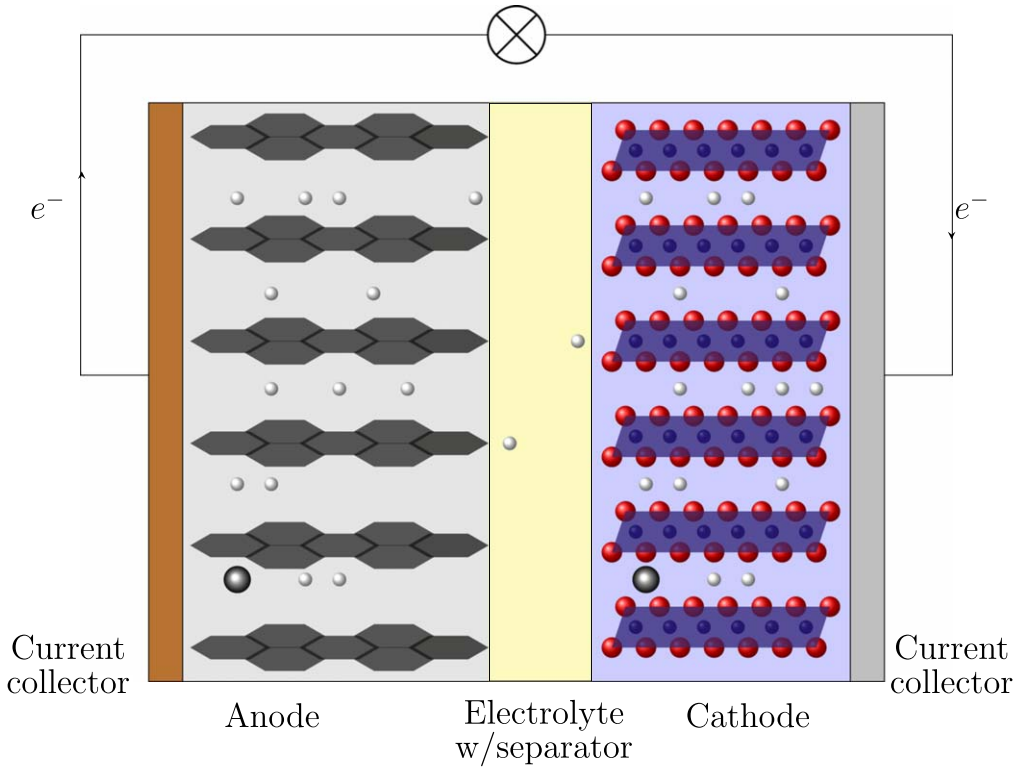

Figure 1. Schematic illustration of a graphite | $LiCoO_2$ full-cell.

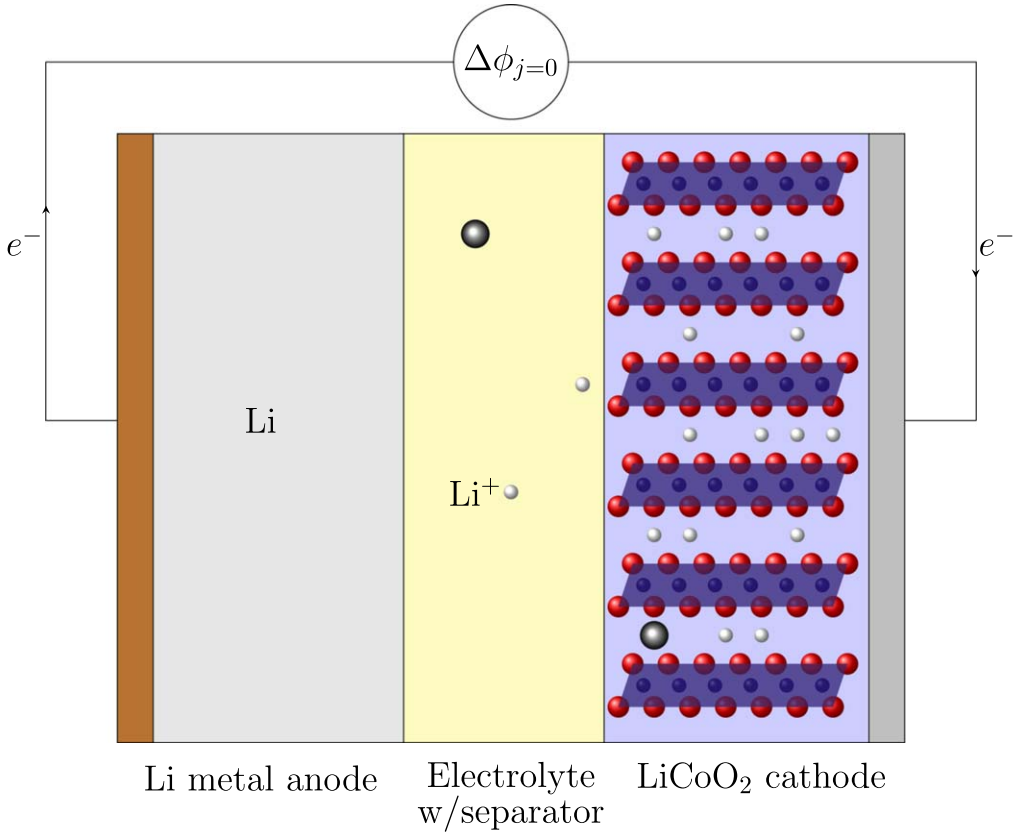

Figure 2. Schematic illustration of a $LiCoO_2$ half-cell.

This review is also meant to help mend this situation, by providing data input for such models.

Our aim is to reveal and localize all LIB reversible heat effects that follow from the theory of non-equilibrium thermodynamics. This theory relates, from Onsager's reciprocal relations,[20] the Peltier heat of an electrode-electrolyte interface to the Seebeck coefficient of a thermoelectric cell with two of the same electrodes.[19] The Dufour or the reciprocal Soret effect can, according to theory, be determined from the approach toward a stationary state in Seebeck coefficient experiments. Thermoelectric cells are therefore particularly useful for the determination of the magnitude and location of reversible heat effects in batteries.[19,25] We shall review literature published on this topic over the last 30 years, to help set a basis for further research.

The schematic structure of a cell used for Seebeck coefficient determinations is shown in Fig. 3, using Li-metal electrodes as an example. The cell potential at open circuit conditions, or the *emf* which we will call it, is measured with identical electrodes (top and bottom), and held at different temperatures by circulating thermostatted water or by Peltier elements.[21] The cell in question consists of two lithium metal electrodes separated by an inert, micro-porous separator film soaked with a LIB electrolyte. The heating is from the top, in order to avoid convection in the liquid electrolyte during measurements.[26] This cell will directly provide Peltier heats for the anode reaction.

The electrolyte of the thermoelectric cell has frequently more than one component. When this is the case, a Soret effect will take place. This means that there is a separation of components in the thermal field.[19,20] Diffusion will occur superimposed on charge transfer, see Eq. 5b. The rise of a concentration gradient will be reflected in the measured *emf*. Until Soret equilibrium has been reached (all mass fluxes are zero), the measured *emf* will vary with time. More than two components in the electrolyte can complicate the situation.[16] The *emf* of the initial and stationary states can differ widely.[16] The difference gives information on the Soret effect or the heats of transfer in the electrolyte. The stationary state value is needed to predict of the time variation of the interface temperature in LIBs.[11] We shall argue that it is important to continue to measure the thermoelectric potential beyond the initial state until a stationary state has been reached.

In the LIB community, the electrode where the anodic reaction takes place during discharge, is often referred to as the anode at all times, and similarly for the cathode. Here, we are dealing with heat effects that are changing sign with the direction of the electric current. To our purposes it is therefore more accurate to use the terms anode and cathode in the traditional sense, to mean the electrode where the oxidation and reduction reaction take place, respectively.

The immediate objective of the review is thus three-fold. We will

(i) provide an overview of earlier experiments relevant for LIB; i.e. full- and half-cell- entropies, as well as Seebeck coefficient measurements.
(ii) show how to determine a cathode Peltier heat from a Seebeck coefficient of an anode and the cell's entropy change.
(iii) present results of such computations for several electrodes with varying lithium content used in LIB. We shall thus provide new data-sets that can be used to improve today's lithium-ion battery thermal modelling efforts.

We limit the review to measurements on thermoelectric cells relevant for LIB electrodes. For an extensive review on the history of thermoelectric cells, we refer to the work of Agar,[27] Quickenden et al.[28] and Gunawan et al.[29]

The review is organized as follows. A review of full- and half-cell entropies is first presented. We next discuss how to measure the relevant Seebeck coefficients and compute the Peltier heat. The main equations needed to describe the thermoelectric cell in Fig. 3 are given,[11] with emphasis on lithium metal electrodes. For details on intercalation electrodes, see Spitthoff et al.[11] Supplementary Material. Experiments with lithium metal electrodes are next reviewed and tabulated. The results are finally used to allocate new Peltier heats to various electrode materials when they function as anodes. We discuss the reliability of these Peltier heats and data missing in literature.

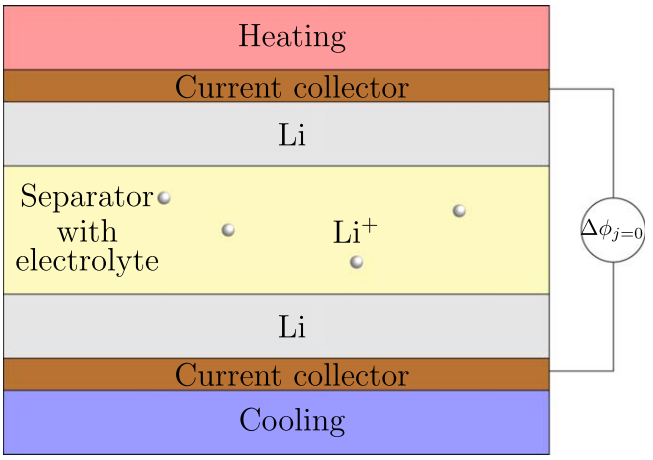

Figure 3. Schematic illustration of a thermoelectric cell, used to measure the Seebeck coefficient. The *emf* is measured between two lithium electrodes, thermostated at different temperatures. A filter filled with electrolyte separates the electrodes.

The Entropy of the Battery Reaction and the Reversible Heat Effect

This Section gives the history of cell entropy measurements in LIB cells, starting with the pioneering studies and ending with cornerstone half-cell measurements. An overview of the results are given in Tables IIa–IIf. The results will later be combined with Seebeck coefficient measurements with lithium electrodes, to calculate battery electrode Peltier heats, see below.

Full-cell and half-cell entropy measurements.—According to classical thermodynamics, the entropy change of an electrochemical cell is given by the temperature dependence of the *emf* :[30,31]

$$\Delta S = nF\frac{d}{dT}\Delta_{tot}\phi_{j=0} \qquad [1]$$

Here n is the number of electrons involved in the electrode reaction, F is Faraday's constant, T is the temperature of the isothermal cell and $\Delta_{tot}\phi_{j=0}$ is the cell *emf*, measured in an open circuit, when the electric current density $j \approx 0$. The more common symbol for the *emf* is E. The entropy change is associated with the reversible heat effect due to the electrode reactions:

$$q = \frac{T\Delta S}{nF}j \qquad [2]$$

where q is the total reversible heat produced per unit of time in the cell. The entropy change in a battery can be determined from this heat effect.[32] In a non-equilibrium thermodynamic description, the local entropy balance at the electrode surfaces enters via the Peltier heat. We showed in the Supplementary material of Spitthoff et al.[11] how the local reversible heat effect at the two electrode surfaces in LIBs add to the total reversible heat effect under isothermal conditions.

As mentioned in the Introduction, it is customary in the battery literature to speak of a battery as a "full-cell", while a "half-cell"

refers to a cell where one of the electrodes in the battery is replaced by a lithium metal electrode, cf. Figs. 1 and 2. Equation 1 applies to full- as well as half-cells. The terminology 'half-cell' may unfortunately point to properties of one electrode only. We shall nevertheless use the name here, but always refer for clarification to the experiment done, see below for more details.

The total reversible heat effect, the entropy change of the full-cell battery with a typical anode and cathode chemistry, has been obtained with help of Eq. 1. It has been proposed that full-cell entropy changes can be estimated from half-cell entropy changes.[15,33] There has been a number of reports on half-cell entropy changes.[34–38] Zhang et al. reviewed potentiometric methods in use to find the reaction entropy of LIBs.[39] The typical experimental set-up[40] thermostats the cell, either using a water bath[34] or using a thermostatting chamber.[40,41] The outer cell temperature is then controlled, for instance by attaching a thermocouple to the connecting lead. If the measurement is done at different states of charge (SoC), the cell is discharged/charged using a battery tester. Once the desired SoC has been reached, ideally the cell is allowed to reach a stable *emf*. In practice, a trade-off is made between the waiting time in practice for a stable reading of the *emf* and the wanted accuracy of the measurement.[39,42] The *emf* is measured at different set temperatures, and the cell is re-thermostatted after each temperature change. For further details on the experimental techniques for measuring entropy we refer to the review by Zhang and co-workers.[39] For details on calorimetric measurements, see for instance.[32,41]

Full-cell entropy measurements have been done on various cell assemblies, such as pouch cells or cylindrical cells.[40,41] Measurements have also been done on commercial cells.[43,44] Coin cells have often been used in half-cell measurements (Fig. 2).[34,40]

The full-cell entropy change can be obtained from Peltier heats for the separate electrode reactions, see below. The electrolyte need be the same for independently determined Peltier heats. The entropy change of the LIB cell in Fig. 2 is *not* equal to the local heat effect of one electrode surface. This is a common misunderstanding in the literature.[6] The reason why is that the local heat effect, the Peltier heat, contains additional terms (see Eq. 19 below). It contains, but is not equal to, the entropy change of the half-cell in Fig. 2. This problem was also addressed in.[11]

Wittingham[45] was first to report the entropy change of LIB half-cells. Experiments were done with Li_xTiS_2 (LTS) electrodes with degree of intercalation, $x \approx 0.6$ and 1. The experiment was followed up by Thompson et al.[46] Dahn et al. and Honders et al. also investigated Li_xTiS_2,[47,48] and obtained results in agreement with those of Whittingham (see Table IIf).[45,46,48] These entropy measurements were aimed to understand the phase diagram of the electrode materials.

Pereira-Ramos and co-workers reported the entropy of insertion of Li into LiV_2O_5 electrodes from potentiometric measurements.[49] They continued to measure the effect of lithium insertion in $LiMn_2O_4$.[50] Prior to this, Popov and co-workers had also studied the thermodynamic properties of lithium insertion into $Li_xV_2O_5$.[51] However, instead of employing half-cells, they only used Li-metal as a reference electrode in the cell Li | 0.5 M $LiClO_4$ in dimethyl sulfoxide | $Li_{0.26}V_2O_5$. They then used $Li_{0.26}V_2O_5$ as a reference in the cell $Li_{0.26}V_2O_5$ | 0.5 M $LiClO_4$ in dimethyl sulfoxide | $Li_xV_2O_5$. They estimated the *emf* of this half-cell, and also the *emf* of the $Li_{0.26}V_2O_5$ half-cell, to ascertain the properties of the reference electrode.

Hallaj and co-workers reported the potentiometric and calorimetric measurements of the entropy change of a commercial cell. Their purpose was to find the reversible heat effects in LIBs.[52] The reversible heat effect was connected to the cell entropy change by the temperature, see e.g.,[31] and Eq. 1. The overall effect was early taken into account in thermal modelling of batteries at large,[5,53,54] but had so far been neglected for LIBs. One explanation can be lack of data. An exception was the investigation of the primary lithium metal battery Li-$SOCl_2$.[55] Hallaj et al. followed up on this by reporting entropy measurements on commercial cells as well as the graphite half-cell.[44] This first report on the graphite half-cell entropy was, unfortunately, only done for a few lithiated states. The amount of lithium that was intercalated in graphite, was only indirectly stated through the *emf* -value of the half-cell. This lack of accuracy in the measurement of the graphite half-cell was later amended by Thomas et al. and Reynier et al.[35,37]

Saito et al. investigated heat effects in a commercial $LiCoO_2$|hard carbon cell by calorimetry. Endothermic effects were observed, which can only be attributed to reversible heat effects.[56] The group followed up with a study on entropy changes in commercial cells with LCO, $LiNi_{0.7}Co_{0.3}O_2$ (NC), and $LiMn_2O_4$ (LMO) as cathode materials during discharge and graphite, hard carbon and hybrid carbon as anode materials.[41]

The full-cell and half-cell entropy changes of LCO and mesocarbon microbead graphite was studied by Koboyashi et al.,[9] by measuring the heat flows during charge and discharge. The group attributed the thermal characteristic behavior to the electrodes of the half-cell measurements; clearly stating that the contribution from the lithium metal electrode could not be determined from these experiments. The Li-metal was correctly thought to contribute a constant off-set to the entropy measurement. Despite this, they erroneously concluded that the negative heat effects observed in the graphite (Li_xC_6) half-cell for some x-values meant that the lithium intercalation into graphite was endothermic for specific SoC values. Doing this, they forgot their observation of an undetermined contribution from Li-metal. The same erroneous conclusion was also drawn by Lu et al.[57] We shall return to this in the discussion.

Onda and co-workers measured entropy changes, both through the temperature variation of the *emf* and through the difference of the heat generated during charging and discharging of commercial LCO|hard carbon and LCO|graphite cells.[32] The entropy data and the differences between the two carbonaceous electrode showed the same trend as the corresponding data of Saito et al.[56]

Thomas et al. reported the half-cell entropy of cells with anodes of LMO, $LiNi_{0.8}$ $Co_{0.2}$ O_2, $LiCoO_2$ and, as already stated, graphite half-cells for the full state-of-charge spectrum.[34,35] Reynier et al. also reported the half-cell entropy for electrodes of LCO, graphite, disordered carbonaceous materials, and carbons with varying degrees of graphitization[37,38,58,59] cf. Fig. 2. These studies were done on electrodes that are extensively used in commercial cells today with the common electrolyte $LiPF_6$ dissolved in EC:DMC. The lithium content was also well defined. The values found by the two mentioned groups, as well as others, were also fairly consistent. This lends credence to all values reported in Fig. 5 and Tables IIa and IIb.

Viswanathan et al. reported full- and half-cell entropies measurements with electrodes lithium iron phosphate, $LiFePO_4$ (LFP), and lithium titanate, Li_2TiO_3. They compared with half-cell entropies found in literature and computed from this estimates of full-cell entropies.[15] Kai et al. investigated the effect of particle size on the half-cell entropy of LFP.[60]

We have seen from the literature survey above that particular emphasis can be put on Peltier heats that are calculated from the entropy data of Thomas et al. and Reynier et al.[35,37] These and additional works on measurements of cell entropy changes of half-cells are summarised in Tables IIa–IIf below. They represent an untapped source for Peltier heat calculations, as will be shown in detail later.

Half-cell and Peltier heat measurements.—The name "half-cell" has also been used in the electrochemical literature to name an electrode| electrolyte interface.[61] To avoid confusion with the nomenclature in the preceding section, we shall refer to this interface region as "a single electrode interface". For the lithium-metal | electrolyte -single electrode, the anode reaction is:

$$Li \rightarrow Li^+ + e^- \qquad [3]$$

The heat that can be associated with this reaction, is a local reversible heat effect, given by the single electrode Peltier heat,

$\pi^{s,i}$ where i = a or c refers to anode or cathode interfaces, and s to the surface. This Peltier heat will be defined by the entropy balance over the interface region (see below). The entropy added in the form of heat must compensate for the entropy that is liberated by disappearance of lithium, the entropy transported away by electrons in the electrode, as well as the entropy transported by lithium ions into the electrolyte.

A common misconception is that the single electrode Peltier heat can be found from the temperature variation of a half-cell (see Fig. 2),[6] or that the local heat generation can be found from the entropy change of the half-cell in Fig. 2.[17] The half-cell in LIB terminology, does not connect to a single electrode.

It can be shown on theoretical grounds that the entropy change of a cell in general is equal to the difference between single electrode Peltier heats of the electrodes used.[5,19] We obtain:

$$T\Delta S = \pi^{s,a} - \pi^{s,c} \qquad [4]$$

We shall see below that electrolyte terms enter both Peltier heats in such a way that they cancel in ΔS. The electrolyte term contributes to the local effect, however. This is the reason why the Peltier heat differ from the entropy change of a half-cell. Equation 4 suggests that the Peltier heats need not be smaller than the cell entropy change. If one of them is small, the other may still be large. We shall see later in the review that this is indeed the case.

Thermoelectric Cell Theory

Gunnarshaug et al.[16] derived the Seebeck coefficient of a LFP thermoelectric cell with ternary electrolyte and two identical electrodes. Their derivations included all reversible heat effects. The theory that we need, is thus available, so we repeat only the outcome of their derivations and the assumptions involved. Expressions that apply to cells with aqueous electrolytes and pure metal electrodes[21,27] are not sufficient.

In the measurement illustrated in Fig. 3, a temperature difference is applied to the cell in the direction normal to the electrode surfaces. Only one-dimensional transport processes need be considered. We follow the terminology from Kjelstrup and Bedeaux,[20] which for clarity is also illustrated in Fig. 4. For further details on the measurement of Seebeck coefficients of LIB materials, we refer to our previous work.[8,16]

Three steps lead to the expression for the Seebeck coefficient that is measured in the apparatus in Fig. 3. The first step is to find the entropy production of each cell layer or interface. The next step is to determine the constitutive equations of transport. In the final step the proper equation is integrated with the boundary conditions of the experiment, or the process, to give the relation between the *emf* and the temperature difference. For the complete derivation we refer to.[11,16]

We recapitulate for illustration the outcome of step 2 for the electrolyte. The flux-force equations are:

$$J_q' = -\lambda\frac{\partial T}{\partial x} + \sum_{i=1}^{n-1} q_i^*\left(J_i - \frac{t_i}{F}j\right) + \frac{\pi}{F}j \qquad [5a]$$

$$J_i = -c_i D_{i,T}\frac{\partial T}{\partial x} - \sum_{j=1}^{n-1} D_{ij}\frac{\partial c_j}{\partial x} + \frac{t_i}{F}j \qquad [5b]$$

$$\left(\frac{\partial \phi}{\partial x}\right) = -\frac{\pi}{FT}\frac{\partial T}{\partial x} - \sum_{i=1}^{n-1}\frac{t_i}{F}\left(\sum_{j=1}^{n-1} a_{ij}\frac{\partial \ln c_j}{\partial x}\right) - rj \qquad [5c]$$

The properties are defined as follows.

- J_q' is the measurable heat fluxλ
- is the thermal conductivity at stationary state,
- q_i^* is the heat of transfer of component *i*. The property which is linked to the Dufour effect is defined as $q_i^* = (J_q'/J_i)_{dT=0,j=0,J_{j\neq i}=0}$,
- J_i is the mass flux of (neutral) component *i*,
- t_i is the transference coefficient of component *i*,
- π^k is the Peltier coefficient of material k defined by $\pi^k = (J_{qF/j}')_{dT=0,J_j=0}$ (not to be confused with $\pi^{s,i}$),

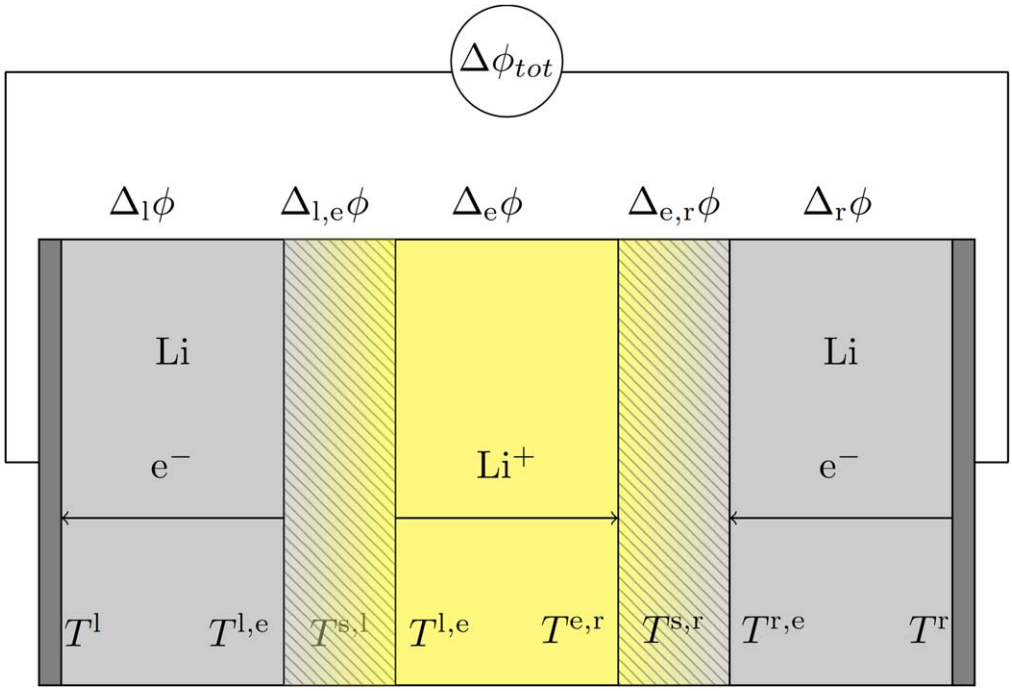

Figure 4. Notation used in the theory of thermoelectric cells. Symbols a,e,c are used for anode, electrolyte, cathode. Superscripts i, j indicate phase i next to phase j. The symbol Δ means a difference taken between the right hand side- and the left hand side value. Two lithium reversible electrodes are used. Charge is conducted in the electrolyte by Li^+ only (anion frame of reference).

- c_i is the concentration of component i,
- $D_{i,T}$'s are the thermal diffusion coefficients,
- D_{ij}'s are interdiffusion coefficients (generalised Fick diffusion coefficients),ϕ
- is the electric potential,
- a_{ij} is a coefficient relating the chemical potential gradients evaluated at constant temperature as linear combination of concentration gradients, and
- r is the electric resistivity.

Similar relations can be written for each of the electrode surfaces, see.[16]

The Seebeck coefficient.—The last step is to integrate equations like 5c for each phase, and relate the electric potential to the thermal driving force. The ratio gives a contribution from each phase to the Seebeck coefficient of the cell in Fig. 3. The integration is carried out for *emf* conditions (open circuit, $j = 0$), in the start of the experiment, at $t = 0$, and at Soret equilibrium, when $J_i = 0$ at stationary state, $t = \infty$.

Contributions from the bulk electrodes.—Each metal electrodes in Fig. 3 is kept at uniform temperature (lithium metal has a high thermal conductivity). On the left-hand side, $T^{\mathrm{l}} = T^{\mathrm{l,e}}$, and on the right-hand side, $T^{\mathrm{r}} = T^{\mathrm{r,e}}$. By integrating from the potentiometer to the electrode surface on both sides, we obtain the following contributions to the Seebeck coefficient:[16]

$$\frac{\Delta_{\mathrm{l}}\phi + \Delta_{\mathrm{r}}\phi}{\Delta_{\mathrm{l,r}}T} = -\frac{\pi}{TF} \qquad [6]$$

where $\Delta_{\mathrm{l,r}}T = T^{\mathrm{r}} - T^{\mathrm{l}}$. For terminology, see Fig. 4. There are no concentration gradients in the electrodes of pure lithium. The Peltier coefficient expresses a reversibly transported heat. It is therefore connected to the transported entropy of the electron, $S^*_{\mathrm{e}^-}$, in the electrode material

$$\pi = TS^*_{\mathrm{e}^-} \qquad [7]$$

Contributions from the electrode reactions.—At the left hand side surface lithium-metal|electrolyte, we have the anodic reaction, as given in Eq. 3. At *emf* conditions with thermostatted electrodes, the electric potential jump at the electrode is given by Nernst' expression.

$$(\Delta_{i,o}\phi)_{j=0} = -\frac{\Delta_n G^{\mathrm{s}}}{F}$$

where $\Delta_n G^{\mathrm{s}}$ is the Gibbs energy of the neutral component in Eq. 3.[a] For the left-hand side reaction:

$$\Delta_n G^{\mathrm{s}} = -\mu_{\mathrm{Li}}(T^{\mathrm{l}}) = -H_{\mathrm{Li}}(T^{\mathrm{l}}) + T^{\mathrm{l}}S_{\mathrm{Li}} \qquad [8]$$

where μ_{Li} is the chemical potential, H_{Li} is the molar enthalpy, and S_{Li} is the molar entropy of pure lithium. For the right-hand side, we have

$$\Delta_n G^{\mathrm{s}} = \mu_{\mathrm{Li}}(T^{\mathrm{r}}) = H_{\mathrm{Li}}(T^{\mathrm{r}}) - T^{\mathrm{r}}S_{\mathrm{Li}} \qquad [9]$$

The contribution from the two electrode surface reactions is then:

$$\frac{\Delta_{\mathrm{l,e}}\phi + \Delta_{\mathrm{r,e}}\phi}{\Delta_{\mathrm{l,r}}T} = \frac{S_{\mathrm{Li}}}{F} \qquad [10]$$

This applies to an electrode of lithium metal. For electrodes with intercalated lithium, $\mathrm{Li}_x - \Theta$, where Θ is the host structure, the expression contains the partial molar entropy.[16] The partial molar entropy of intercalated lithium, $S_{\mathrm{Li(x)}}$, was called the excess partial molar entropy of Li by Thompson.[46] The entropy depends on the degree of intercalation of lithium x. For the partial molar entropy, the ideal expression has been used.

$$S_{\mathrm{Li(x)}} = S^0 - R\ln x \qquad [11]$$

where S^0 is the entropy of the standard state. The term (1-x) has also been included, to account for unoccupied positions in the host structure.[46]

Electrolyte contribution.—The battery elecrolyte has a solute, typically lithium hexafluoro-phosphate ($\mathrm{LiPF_6}$), and a solvent which may contain several organic carbonates, such as propylene carbonate (PC), ethylene carbonate (EC), dimethyl carbonate (DMC) and diethyl carbonate (DEC). The electrolyte is soaked into an inert separator keeping the electrodes apart. The salt and solvent will separate in a thermal gradient (the Soret effect). The concentration gradients that arise, will affect the value of the Seebeck coefficient. By measuring before ($t = 0$) and after ($t = \infty$) the gradient is established, we can examine this effect.

By integrating across the thickness of the electrolyte, we find the general contribution from the electrolyte to the Seebeck coefficient:

$$\left(\frac{\Delta_{\mathrm{e}}\phi}{\Delta_{\mathrm{e}}T}\right)_{j=0} = -\frac{S^{*,\mathrm{e}}_{\mathrm{Li}^+}}{F} - \sum_{i=1}^{n-1}\frac{t_i q_i^{*,\mathrm{e}}}{TF} - \sum_{i,j=1}^{n-1}\frac{t_i^{\mathrm{e}}}{F}a_{ij}\frac{\Delta_{\mathrm{e}}\ln c_j}{\Delta_{\mathrm{e}}T} \qquad [12]$$

The time dependence of the Seebeck coefficient is contained in the final term, and is caused by the Soret effect, as explained. At $t = 0$, the last term is zero, and we obtain

$$\left(\frac{\Delta_{\mathrm{e}}\phi}{\Delta_{\mathrm{e}}T}\right)_{j=0,t=0} = -\frac{S^{*,\mathrm{e}}_{\mathrm{Li}^+}}{F} - \sum_{i=1}^{n-1}\frac{t_i q_i^{*,\mathrm{e}}}{TF} \qquad [13]$$

In the electrolyte, entropy (heat) is transported with the charge carrier, the ion Li^+, but heat can also also be transported with neutral components of the electrolyte, as heats of transfer, q_i^*, cf. Eq. 5a.[16,62]

At stationary state the second term on the right-hand side of Eq. 12 cancels the third (by introducing the Soret equilibrium condition), leaving only the contribution from the transported entropy.

$$\left(\frac{\Delta_{\mathrm{e}}\phi}{\Delta_{\mathrm{e}}T}\right)_{j=0,t=\infty} = -\frac{S^{*,\mathrm{e}}_{\mathrm{Li}^+}}{F} \qquad [14]$$

The following Peltier coefficients apply here:

$$\pi^{\mathrm{e}}_{t=0} = TS^*_{\mathrm{Li}^+} + \sum_{i=1}^{n-1} t_i q_i^* \qquad [15]$$

$$\pi^{\mathrm{e}}_{t=\infty} = TS^*_{\mathrm{Li}^+} \qquad [16]$$

Equation 15 shows that the Seebeck coefficient depends on the electrolyte. This is why an expression for a binary electrolyte is not applicable for ternary electrolytes. The heat of transfer, the transference coefficient and the transported entropy of lithium ions all depend on the electrolyte composition.

Seebeck coefficients.—We can now find the total Seebeck coefficient of the cell in Fig. 3 by adding contributions from the bulk electrode phases, the electrode surface reactions, and the

[a]For expression in terms of Maxwell potential, see.[20]

electrolyte, at $t = 0$ and $t = \infty$:

$$\left(\frac{\Delta_{\text{tot}}\phi}{\Delta T}\right)_{j=0,t=0} = \frac{1}{F}(S_{\text{Li}} - S^*_{\text{e}^-} - S^*_{\text{Li}^+} - \sum_{i=1}^{n-1}\frac{t_i q_i^*}{T}\Bigg) \quad [17]$$

and

$$\left(\frac{\Delta_{\text{tot}}\phi}{\Delta T}\right)_{j=0,t=\infty} = \frac{1}{F}(S_{\text{Li}} - S^*_{\text{e}^-} - S^*_{\text{Li}^+}) \quad [18]$$

These are expressions we can use to decompose data from Seebeck coefficient measurements.

The electrode interface as a heat source or sink.—In the expressions of the Seebeck coefficient above, we identified and used the Peltier coefficients of the bulk electrode, of the surface reaction, and of the electrolyte. When the Thomson effect is negligible, there is no reversible heat change along the conductor. Reversible heat effects are then manifested only at the junctions. These effects are now in focus.

The *Peltier heat of an interface* (a junction), $\pi_t^{\text{s,i}}$, is related to the heat change associated with transport of charge across the interface. There is always a change in charge carrier connected with the electrochemical reaction. A Peltier heat can therefore be expected. The Peltier heat is defined as the heat that we need to add to the junction in order to keep its temperature constant, when one faraday of charge is passing the junction from the left to the right-hand side of the junction.[19]

We find the Peltier heat of the junction from the entropy balance at the junction. It becomes equal to the difference of the *Peltier coefficients* of the bulk phases right and left of the interface plus the contribution from the electrochemical reaction. In our case, this balance is at $t = 0$:

$$\pi^{\text{s,a}}_{t=0} = \pi^{\text{e}} - \pi^{\text{a}} - TS_{\text{Li}} = -(TS_{\text{Li}} - TS^*_{\text{Li}^+} - TS^*_{\text{e}^-} - \sum_{i=1}^{n-1} t_i q_i^*) \quad [19]$$

while at stationary state, we obtain:

$$\pi^{\text{s,a}}_{t=\infty} = -(TS_{\text{Li}} - TS^*_{\text{Li}^+} - TS^*_{\text{e}^-}) \quad [20]$$

Superscript s,a is used to show that the Peltier heat is an interface or surface property, here associated with the anode. We see from Eqs. 17–20 that the Peltier heat is related to the Seebeck coefficient:

$$\pi_t^{\text{s,a}} = -T\left(\frac{\Delta_{\text{tot}}\phi}{\Delta T}\right)_{j=0,t} \quad [21]$$

The origin of the relationship is an Onsager relation. It allows us to find the Peltier heat via the more precise measurement of the Seebeck-coefficient. We refer to the initial state and the stationary state, using $t = 0$ and $t = \infty$. The expression above applies to the junction of the anode. (The entropy balance refers to electric charge that is passing from left to right in the internal circuit.) The sign of the Peltier heat changes if we change the direction of the electric current. The values tabulated for the Peltier heat in this review refers thus to its use as an anode. A cathode surface of the same material, will then have a Peltier with the opposite sign. We refer to[11] for information on the Peltier heat of the cathode is implemented in a thermal model.

The Peltier heat can also be measured directly by calorimetry, as suggested by the definition of the coefficients, but it is clearly difficult to measure a heat effect at near isothermal conditions. Therefore, we take advantage of the relation given to us by non-equilibrium thermodynamic theory, between the Peltier heat and the Seebeck coefficient. The Peltier heat of a lithium metal electrode surface, was here obtained from the Seebeck coefficient in Eq. 17.

The difference between the two Peltier heats of an electrode gives a direct link to the heats of transfer:[19,27]

$$\pi^{\text{s,a}}_{t=0} - \pi^{\text{s,a}}_{t=\infty} = \sum_i^{n-1} t_i q_i^* \quad [22]$$

This explains why both states, $t = 0$ and $t = \infty$, are needed for thermal modelling. The stationary state value is perhaps more relevant for modelling, for instance because the battery operates in a quasi-stationary state. We return to this remark in connection with Eq. 24. The difference between the initial and stationary state value can be substantial,[16] in direct contradiction to claims of other research groups.[63] The Peltier heat does not depend on the frame of reference that is chosen for the fluxes, but the mass fluxes and transference coefficients do, see.[62] There are $n - 1$ independent fluxes of neutral components in the electrolyte, and the sum in Eq. 22 is carried out over $n - 1$, where the n'th component serves as the frame of reference.

Further comments on the sign convention.—When the entropy change of the cell reaction is positive, it contributes to work production. Heat is then extracted from the surroundings and transformed to electric work. The statement applies also to a single electrode. The sign of the Peltier heat is by definition the same as that of the electric potential jump produced at the electrode (Nernst equation). When the electrode reaction contributes to work done, the potential jump as well as the Peltier heat are positive.

The Peltier heat tabulated in the last part of this review refers to an anodic reaction (oxidation), cf. 19. When this value is positive, there is a sink for heat at the anode; it will cool.

The effect is reversible, as the electric current can be reversed. When the same material is performing as a cathode, the nearby region will heat. The minus sign of the last term of Eq. 4 refers to an electrode when reduction occurs, where the electrode serves as a cathode. When the Peltier heat of the anode, is numerically larger than that of the cathode, the cell reaction entropy is positive from Eq. 4, and contributes to the cell's work. For identical and uniform materials, we have from Eq. 4

$$\pi^{\text{s,c}} = \pi^{\text{s,a}} \quad [23]$$

because $\Delta S = 0$. Recall that the sign of the Peltier heat will here always refer to the anode reaction.

Heubner et al.[17] observed cooling at the LCO electrode in a graphite|LCO -cell during charging, i.e. when LCO was acting as an anode. Simultaneously, they observed heating during cell discharge. This means that the LCO Peltier heat is positive for the anode reaction, as observed also by Richter et al.[24] Maeda measured a cooling effect during lithium de-intercalation in graphite,[64] suggesting that also graphite has a positive Peltier heat for the anode reaction. For this to be possible, Li-metal as an anode must also have a positive Peltier heat (see Table IIb). Huang et al. observed cooling for the lithium metal, but reported a negative Peltier heat, meaning that different sign conventions has been employed.

A remark on battery modelling.—A great effort has been made to model temperature gradients in the LIB, as these can be detrimental for the materials. A first step is then to include all reversible heat effects into a complete model of a single cell.[11] The data discussed in this review are all needed to find a more detailed temperature profile across the battery.

Table I. Measured Seebeck coefficients and computed Peltier heats at 298 K for Li-metal electrodes operating as anodes. Errors are given as two standard deviations.

(a) Pure lithium metal

Authors [References]	Electrode	Electrolyte	$(\Delta\phi/\Delta T)_{j=0,t=0}$ mV K^{-1}	$\pi^{s,Li}_{t=0}$ kJ mol^{-1}
Hudak et al.[a,b) 21]	Li	1 M $LiBF_4$ in PC	-1.07 ± 0.06	30 ± 2
		1 M $LiPF_6$ in PC	-1.24 ± 0.07	36 ± 2
		1 M $LiPF_6$ in 1:1 v% EC:DMC	-1.25 ± 0.12	36 ± 3
Black et al.[a) 22]	Li	1 M $LiClO_4$ in 1:1 DEC:EC	-0.98 ± 0.06	28 ± 2
			-1.00 ± 0.04	29 ± 1
Huang et al.[a,c) 18]	Li	1 M $LiPF_6$ in EC:DMC 1:1 v	-1.17 ± 0.06	34 ± 2

(b) Lithium intercalation electrodes

Authors [References]	Electrode	x	Electrolyte	$(\Delta\phi/\Delta T)_{j=0,t=0}$ mV K^{-1}	$(\Delta\phi/\Delta T)_{j=0,t=\infty}$ mV K^{-1}	$\pi^{s}_{t=0}$ kJ mol^{-1}	$\pi^{s}_{t=0}$
Black et al.[d) 22]	$Li_{3.5}$ $Fe(CN)_6$	—	1 M $LiClO_4$ in 1:1 DEC:EC	-0.57 ± 0.12		16 ± 3	
Hudak et al.[d) 21]	Li_xTiS_2	0	1 M $LiPF_6$ in 1:1 v% EC:DMC	-0.49 ± 0.09		14 ± 3	
		0.2		-1.1 ± 0.8		30 ± 20	
		0.4		-1.16 ± 0.12		33 ± 3	
		0.6		-1.03 ± 0.08		30 ± 2	
		0.8		-1.00 ± 0.12		29 ± 3	
Hudak et al.[d) 21]	Li_xTiS_2	0	1 M $LiPF_6$ in PC	-0.65		19	
		0.2		-1.1 ± 0.8		30 ± 20	
		0.4		-1.11 ± 0.11		32 ± 3	
		0.6		-1.07		30	
		0.8		-1.05 ± 0.14		30 ± 4	
Hudak et al.[d) 21]	Li_xTiS_2	0	1 M $LiBF_4$ in PC	-0.52 ± 0.09		15 ± 3	
		0.2		-1.0 ± 0.8		30 ± 20	
		0.4		-0.96 ± 0.13		28 ± 4	
		0.6		-0.96 ± 0.11		28 ± 3	
		0.8		-0.92 ± 0.12		26 ± 3	
Hudak et al.[d) 21]	Li_xTiS_2	0	0.1 M $LiBF_4$ in PC	-0.35 ± 0.07		10 ± 2	
		0.2		-0.7 ± 0.3		20 ± 9	
		0.4		-0.9 ± 0.2		26 ± 6	
		0.6		-0.83 ± 0.06		24 ± 2	
		0.8		-0.79 ± 0.06		23 ± 2	
Hudak et al.[d) 21]	$Li_xV_2O_5$	0	0.1 M $LiPF_6$ in 1:1 v% EC:DMC	-0.60 ± 0.12		17 ± 3	
		0.2		-0.98 ± 0.10		28 ± 3	
		0.4		-1.06 ± 0.07		30 ± 2	
		0.6		-1.0 ± 0.2		29 ± 6	
		0.8		-0.88		25	
Richter et al. et al.[24]	Li_xCoO_2	1	1 M $LiPF_6$ in 1:1 w% EC:DEC	-2.8 ± 0.3	-1.7 ± 0.2	80 ± 9	49 ± 6
Gunnarshaug et al.[16]	Li_xFePO_4	1	1 M $LiPF_6$ in 1:1 w% EC:DEC	-1.3 ± 0.2	-4.3 ± 0.3	37 ± 4	122 ± 5

a) Seebeck coefficients were reported with a positive value. b) Error given to one standard deviation in original work. c) Error assumed given to one standard deviation in original work. d) Seebeck coefficients were reported with a positive value

As example, we take the expression for the time variation of the electrode-surface temperature of the anode, that arise from the heat effects discussed here. The expression was given to first order accuracy[16]

$$\frac{dT^{s,a}}{dt} = \frac{1}{\rho^{s,a}C^{s,a}}\left(-\lambda_a^{s,a}\Delta_{a,s}T + \lambda_e^{s,a}\Delta_{s,e}T + r^{s,a}j^2 - \sum_{i=1}^{n-1}J_i^{e,a}\mu_i^{s,e} - \frac{\pi^{s,a}_{t=0}}{F}j + \sum_{i=1}^{n-1}q_i^{*,e}\frac{t_i^e}{F}j\right) \quad [24]$$

Here $\rho^{s,a}$ and $C_p^{s,a}$ are the excess density and the heat capacity of the interface. Here $\pi^{s,a}_{t=0}$ is the Peltier heat of the initial state, given in Eq. 19. A similar equation can be written for the cathode, see.[11] The last two terms on the right-hand side of the equation add to give the stationary state Peltier heat, $\pi^{s,a}_{t=\infty}$, as seen in Eq. 22. The temperature change of the surface depend on the particular state. A computation of the surface temperature using the initial state Peltier heat requires knowledge of the Dufour effect. An alternative, limited to stationary state values only, is to use the stationary state Peltier heat.[11] Data are not yet available in the literature for q_i^* and only a

few experiments have been done to measure the stationary state Peltier heat.[16]

Seebeck Coefficients in the Literature

Pioneering works on thermoelectric cells were done by Agar and Breck[26,27] and Tyrrell,[65] see the historic reviews.[28,29] We limit ourselves to review LIB-related studies here and in the next section.

In this section we report measurements of Seebeck coefficients using various lithium reversible electrodes. We apply the theory of the previous section, and compute the Peltier heat of the electrode in question from the relevant Seebeck coefficient listed in Tables Ia and Ib. The electrode and electrolyte conditions are specified in the tables of computed data along with the measured Seebeck coefficients. The Peltier heat corresponding to the Seebeck coefficient is computed and shown in the same table. Results for lithium metal electrodes are given in Table Ia, while Table Ib gives results for other lithium reversible electrodes. The error in the listed numbers is, if nothing else is stated, two standard deviations, see Table headings for more details. The results from this section will be used in the next to compute Peltier heats of other battery electrodes.

Lithium metal electrodes.—Three groups report results for the Li metal electrode, Hudak et al.,[21] Black et al.[22] and Huang et al.[22] All groups used a lithium salt of concentration 1 M. The solvents varied between propylene carbonate (PC), a mixture of ethylene carbonate (EC) and dimethyl carbonate (DMC), EC:DMC, and a mixture of EC and diethyl carbonate (DEC), EC:DEC. In spite of this variation in electrolyte, the computed initial state Peltier heats were all positive, ranging within 28–36 kJ mol^{-1} (see Table Ia).

Huang et al. repeated the experiment measuring the heat flow directly through calorimetry, obtaining also there an endothermic reaction. A current density of 0.1 mA cm^{-2} was used to avoid contributions from irreversible heat effects. For the direct measurement the Peltier heat was determined to be 38 kJ mol^{-1}. An even larger cooling effect than that measured through the Seebeck coefficient was thus observed, despite inevitable contributions from irreversible heat effects and heat losses. We will remind the reader that it is the stationary state Peltier heat which is most relevant for thermal modelling (see Eq. 24), which will include contributions from the Dufour effect.

The largest variation in the Peltier heat can be attributed to the lithium salt. This suggests that the anion has some impact on the Dufour effect or on the transported entropy of the lithium ion. In the calculations that follow, we will use the precise value for the lithium salt in the electrolyte that we have information on. This means that we will use the value of Huang et al.[18] of 34 ± 2 kJ mol^{-1} for $LiPF_6$, and the value of Black et al.[22] of 29 ± 1 kJ mol^{-1} for $LiClO_4$.

Other lithium-reversible electrodes.—Several other lithium-reversible electrodes have been used to measure Seebeck coefficients, with the similar electrolyte as for pure lithium electrodes, and with a varying fraction, x, of lithium in the solid solution of the electrode. Results are shown as a function of x in Table Ib. The computed Peltier heat depended on the composition of the electrode. The results are further illustrated in Fig. 8. The Fig. shows that a large degree of consensus about the composition variation in the data. The variation across the composition range is dramatic, almost 25 kJ mol^{-1}. A local maximum is seen around $x = 0.4$. This has been attributed to a possible phase transitions inside the intercalating compound.[46] Few measurements have lasted until a stationary state has been reached, probably because such experiment can take days.[16]

Honders et al.[48] measured the thermoelectric power of the cells Pt (T)| $Li_xTi_{1.03}$ S_2 |Pt $(T + \Delta T)$, and Pt (T)| $Li_xTi_{1.03}$ S_2 (T)| 1 M $LiClO_4$, PC (T) |$Li_xTi_{1.03}$ S_2 |1 M $LiClO_4$, PC $(T + \Delta T)$ |$Li_xTi_{1.03}$ S_2 $(T + \Delta T)$| Pt $(T + \Delta T)$. When we describe the last cell set-up with the theory presented above,[20] we find that the Seebeck coefficient of the complete cell is equal to the partial molar entropy of lithium, $S_{Li(x)}$. Their set-up offers therefore a possible way to measure the entropy of intercalated lithium, here in LTS.

Kuzminskii et al.[23] reported the first Seebeck coefficient in a cell made from LIB materials. In 1994, the group reported the initial state Seebeck coefficient of the cell $Li_xTiS_2(T)$| $LiBF_4$, γ-butyrolactone | Li_xTiS_2 $(T + \Delta T)$ for mole fractions of x between 0.1 and 0.9. Few experimental data were reported. Confusingly, the sign convention was not stated, and two conventions were used, but several sets of data were reported.[23]

Huang et al. reported initial state Peltier heats of LCO and graphite electrodes at 100% state-of-charge (SoC). Additionally, they were first to report the initial Seebeck coefficient of a Li metal and a LIB electrolyte thermoelectric cell.[18] The group used the cell Li (T)| 1 M $LiPF_6$ EC:DMC | Li $(T + \Delta T)$. The Seebeck coefficient was 1.17 mV K^{-1}, giving a Peltier heat of -34 kJ mol^{-1}. This refers to an endothermic oxidation reaction, however, suggesting that the Peltier heat is 34 kJ mol^{-1} with our sign convention. The initial state Peltier heat of LCO and graphite was found indirectly through measurement of ΔS of half-cells (see above) and the Peltier heat of Li, analogous to how we determine Peltier heats of other electrode materials later in the text.

Nearly two decades after the report of Kuzminsii et al.,[23] Hudak et al. followed up on their experiment. They measured the initial state Seebeck coefficient with LTS electrodes, for x-values between 0 and 0.8. They reported results for the salts $LiPF_6$ in EC:DMC, for $LiPF_6$ in PC and $LiBF_4$ in PC,[21] see Table Ib. The group investigated electrodes with and without carbon coating. They measured the Seebeck coefficient of cells with Li- metal and LiV_2O_5 electrodes. The variation in the Seebeck coefficient due to varying x is due to changes in the partial molar entropy of lithium in the anode (see Eq. 17). We apply the sign convention presented above with Eq. 17, using ΔS-values for the LTS half-cell[46] (see Table Ib), and find that the variation in the Seebeck coefficients is reflected in the change of the half-cell entropy. We conclude that the values from Hudak et al.[21] give positive Peltier heats for LTS, LiV_2O_5 as well as Li-metal electrodes. We also report this in Table Ib.

Black et al.[22] measured the initial state Seebeck coefficient of the cell Li (T) | 1 M $LiClO_4$ EC:DEC | Li $(T + \Delta T)$. Positive Seebeck coefficients were obtained; 0.98 ± 0.06 and 1.00 ± 0.04 mV K^{-1} (uncertainty of two standard deviations), respectively. The authors used stepped and pulsed gradient methods. In the stepped gradient method, a temperature difference was applied for 1000 seconds and increased/decreased in steps. This was done for around 10 000 s, i.e. 10 steps. In the pulsed gradient method, the temperature difference was applied for 600 seconds and then set to zero for the same amount of time. The first set-up would allow the Soret effect to influence the results more, the longer the experiment is run, creating less defined conditions for analysis.

Schmid et al.[63] reported Peltier heats measured directly by calorimetry during deposition of Li-metal. This was done by placing a sensor on the back side of a working electrode of Ni. The calorimetric method is directly connected to the definition of the Peltier heat (see[66]), but is more prone to errors. The Peltier heat produces a heat source at a particular location, namely the interface, but the thermal conductivity of metal electrodes is very high, and any temperature rise may be hard to record. A calorimetrically determined value will therefore always be a low estimate, because of leaks to the surroundings. For further discussion regarding direct measurement of Peltier heats, see.[65,66] A positive Peltier heat was reported for the deposition reaction, i.e. meaning that Li-metal would cool, when acting as a cathode. This disagrees with the endothermic effect for lithium dissolution reported by Huang et al.[18] Schmid et al.[63] concluded that lithium plating would result in a local cold spot. But other authors have concluded that lithium plating leads to a temperature rise.[67] Schmid et al.[68] reported also a positive Peltier heat for a cell with lithium intercalation in graphite, i.e. when graphite acts as a cathode. This is in conflict with other reports in the

Table II. Entropy change for half-cells at 298 K. The Peltier heat of the lithium metal electrode operating as anode, $\pi^{s,Li}_{t=0}$, is given in Table Ia. Errors are given as two standard deviations, unless otherwise stated.

(a) $LiCoO_2$ electrode

Authors [References]	$\pi^{s,Li}_{t=0}$ kJ mol^{-1} [References]	Electrode	x	Electrolyte	ΔS J K^{-1} mol^{-1}	$\pi^{s,LCO}_{t=0}$ kJ mol^{-1}	$\pi^{s,LCO}_{t=\infty}$ kJ mol^{-1}
Reynier et al.[a) 58]	29 ± 1 [22]	Li_xCoO_2	0.49	1 M $LiClO_4$ in PC	−23 ± 2	36 ± 1	—
			0.5		−29 ± 1	38 ± 1	—
			0.51		−39 ± 1	41 ± 1	—
			0.55		18 ± 2	24 ± 1	—
			0.61		−22 ± 1	35 ± 1	—
			0.72		−35 ± 1	40 ± 1	—
			0.82		−55 ± 1	46 ± 1	—
			0.9		−58 ± 2	46 ± 1	—
			1		−44 ± 2	42 ± 1	—
Thomas et al.[35]	34 ± 2 [18]	Li_xCoO_2	0.54	1 M $LiPF_6$ in 1:1 EC:DMC	−32	44 ± 2	129 ± 7
			0.56		−54	50 ± 2	134 ± 7
			0.58		8	32 ± 2	117 ± 7
			0.61		29	25 ± 2	110 ± 7
			0.63		−9	37 ± 2	122 ± 7
			0.65		−20	40 ± 2	125 ± 7
			0.70		−26	42 ± 2	127 ± 7
			0.77		−34	44 ± 2	127 ± 7
			0.85		−50	49 ± 2	132 ± 7
			0.99		−61	52 ± 2	135 ± 7
Huang[b) 18]	34 ± 2 [18]		∼0.5	1 M $LiPF_6$ in EC:DMC 1:1 v	−8.9 ± 0.6	36 ± 2	121 ± 7
Honders et al. [48]	29 ± 1 [22]	Li_xCoO_2	0.95	1 M $LiClO_4$ in PC	−51.6	44 ± 1	—

(b) Entropy change for a half-cell with LiC_6 as electrode and $LiPF_6$ as solute at 298 K.

Authors [References]	$\pi^{s,Li}_{t=0}$* kJ mol^{-1} [References]	Electrode	x	Electrolyte	ΔS J K^{-1} mol^{-1}	$\pi^{s,C}_{t=0}$ kJ mol^{-1}	$\pi^{s,C}_{t=\infty}$ kJ mol^{-1}
Reynier et al.[37]	34 ± 2 [18]	Li_xC_6	0	1 M $LiPF_6$ 1:1 v% EC:DMC	62	15 ± 2	100 ± 7
			0.1		5	33 ± 2	118 ± 7
			0.2		−4	34 ± 2	119 ± 7
			0.3		−11	37 ± 2	122 ± 7
			0.4		−14	38 ± 2	123 ± 7
			0.5		−14	38 ± 2	123 ± 7
			0.6		−4	35 ± 2	120 ± 7
			0.8		−6	34 ± 2	119 ± 7
			1		−18	39 ± 2	124 ± 7
Reynier et al.[36]	34 ± 2 [18]	Li_xC_6 (Natural graphite)	0	1 M $LiPF_6$ 1:1 v% EC:DMC	62	15 ± 2	100 ± 7
			0.03		38	22 ± 2	123 ± 7
			0.1		3	33 ± 2	118 ± 7
			0.28		−11	37 ± 2	122 ± 7
			0.40		−15	38 ± 2	123 ± 7
			0.47		−14	38 ± 2	123 ± 7
			0.49		−1	34 ± 2	119 ± 7
			0.53		−4	35 ± 2	120 ± 7
			0.69		−5	35 ± 2	120 ± 7
			0.88		−10	37 ± 2	122 ± 7
			0.92		−18	39 ± 2	124 ± 7
Reynier et al.[36]	34 ± 2 [18]	Li_xC_6 (MCMB)	0	1 M $LiPF_6$ 1:1 v% EC:DMC	30	25 ± 2	110 ± 7
			0.03		19	28 ± 2	113 ± 7
			0.11		4	33 ± 2	118 ± 7
			0.19		−5	35 ± 2	120 ± 7
			0.27		−12	37 ± 2	122 ± 7
			0.45		−13	37 ± 2	121 ± 7
			0.49		−7	36 ± 2	121 ± 7
			0.58		−7	36 ± 2	121 ± 7
			0.67		−7	36 ± 2	121 ± 7
			0.77		−11	37 ± 2	122 ± 7

Table II. (Continued).

(b) Entropy change for a half-cell with LiC_6 as electrode and $LiPF_6$ as solute at 298 K.

Authors [References]	$\pi^{s,Li}_{t=0}$* kJ mol^{-1} [References]	Electrode	x	Electrolyte	ΔS J K^{-1} mol^{-1}	$\pi^{s,C}_{t=0}$ kJ mol^{-1}	$\pi^{s,C}_{t=\infty}$ kJ mol^{-1}
			0.004		2.1	33 ± 2	118 ± 7
			0.05		24.8	26 ± 2	111 ± 7
			0.13		3.1	33 ± 2	118 ± 7
			0.20		−4.3	35 ± 2	120 ± 7
			0.27		−16.2	38 ± 2	123 ± 7
Thomas et al.[35]	34 ± 2 [18]	Li_xC_6 (MCMB)	0.44	1 M $LiPF_6$	−15.1	38 ± 2	123 ± 7
			0.50	in 1:1 EC:DMC	−13.0	36 ± 2	121 ± 7
			0.58		−7.2	36 ± 2	121 ± 7
			0.72		−8.3	37 ± 2	122 ± 7
			0.89		−10.8	37 ± 2	122 ± 7
Huang[c) 18]			1	1 M $LiPF_6$ EC: DMC 1:1 v	−21 ± 2	40 ± 2	125 ± 7
			0		44	21 ± 2	—
			0.06		6	32 ± 2	—
			0.23		−4	35 ± 2	—
Jalkanen et al. [d) 33]	34 ± 2 [18]	Li_xC_6	0.29	1 M LiPF6	−13	37 ± 2	—
			0.41	EC:EMC:DMC (1:1:1)	−14	38 ± 2	—
			0.48		−12	37 ± 2	—
			0.69		−1	34 ± 2	—
			0.83		−7	36 ± 2	—
			0.92		−9	36 ± 2	—
			0		37	23 ± 2	—
			0.09		19	28 ± 2	—
			0.17		1	33 ± 2	—
			0.26		−8	36 ± 2	—
Yun et al.[d) 40]	34 ± 2 [18]	Li_xC_6	0.34		−14	38 ± 2	—
			0.43	1 M $LiPF_6$	−15	38 ± 2	—
			0.51	EC:EMC:DMC (1:1:1)	0.5	33 ± 2	—
			0.60		−2	34 ± 2	—
			0.68		−5	35 ± 2	—
			0.77		−13	38 ± 2	—
			0.85		0	34 ± 2	—

(c) $LiNi_xMn_yCo_zO_2$ (NMC), $LiMn_xCo_yO_2$ (MC) and $LiNi_xCo_yO_2$ (NC) electrodes.

Authors [References]	$\pi^{s,Li}_{t=0}$ kJ mol^{-1} [References]	Electrode	x	Electrolyte	ΔS J K^{-1} mol^{-1}	$\pi^{s,el}_{t=0}$ kJ mol^{-1}	$\pi^{s,el}_{t=\infty}$ kJ mol^{-1}
			0.4		1.3	33 ± 2	118 ± 7
			0.49		1.4	33 ± 2	118 ± 7
			0.62		0.2	34 ± 2	119 ± 7
Thomas et al.[35]	34 ± 2 [18]	$Li_xNi_{0.8}\ Co_{0.2}\ O_2$	0.70	1 M $LiPF_6$	0.5	33 ± 2	118 ± 7
			0.80	in 1:1 EC:DMC	−0.8	35 ± 2	120 ± 7
			0.85		−0.8	35 ± 2	120 ± 7
			0.90		−2.1	36 ± 2	121 ± 7
			0.96		0.7	33 ± 2	118 ± 7
			∼0.5		−10.3	37 ± 2	—
			∼0.6		−5.3	35 ± 2	—
Yun et al.[e) 40]	34 ± 2 [18]	$Li_xNi_{0.7}\ Mn_{0.15}\ Co_{0.15}\ O_2$	∼0.65		−7.5	36 ± 2	—
			∼0.75	1 M $LiPF_6$	−6.3	36 ± 2	—
			∼0.85	EC:EMC:DMC	−1.7	34 ± 2	—
			∼0.90	1:1:1 in volume	−1.2	34 ± 2	—
			∼0.95		1.2	33 ± 2	—
			∼1		3.2	33 ± 2	—
			0.35		4	28 ± 1	—
			0.5		−13	32 ± 1	—

Table II. (Continued).

(c) $LiNi_xMn_yCo_zO_2$ (NMC), $LiMn_xCo_yO_2$ (MC) and $LiNi_xCo_yO_2$ (NC) electrodes.

Authors [References]	$\pi^{s,Li}_{t=0}$ kJ mol^{-1} [References]	Electrode	x	Electrolyte	ΔS J K^{-1} mol^{-1}	$\pi^{s,el}_{t=0}$ kJ mol^{-1}	$\pi^{s,el}_{t=\infty}$ kJ mol^{-1}
Kashiwagi et al. [69]	29 ± 1 [22]	$Li_xCo_{0.3}$ $Mn_{1.7}$ O_4	0.6	1 M $LiClO_4$ EC:DEC	7	28 ± 1	—
			0.7		3	28 ± 1	—
			0.9		−18	34 ± 1	—
			0.2		11	25 ± 1	—
			0.3		−1	29 ± 1	—
			0.5		−14	33 ± 1	—
Kashiwagi et al.[69]	29 ± 1 [22]	$Li_xCo_{0.15}$ $Mn_{1.85}$ O_4	0.6	1 M $LiClO_4$ EC:DEC	7	27 ± 1	—
			0.7		1	28 ± 1	—
			0.8		−8	31 ± 1	—
			0.9		−19	34 ± 1	—
			0.1		13	25 ± 1	—
			0.2		6	27 ± 1	—
			0.3		−2	29 ± 1	—
Kashiwagi et al.[69]	29 ± 1 [22]	$Li_xCo_{0.05}$ $Mn_{1.95}$ O_4	0.4	1 M $LiClO_4$ EC:DEC	−13	29 ± 1	—
			0.55		15	24 ± 1	—
			0.75		−10	30 ± 1	—
			0.9		−24	36 ± 1	—

(d) $LiFePO_4$ (LFP) electrodes.

Authors [References]	$\pi^{s,Li}_{t=0}$ kJ mol^{-1} [References]	Electrode	x	Electrolyte	ΔS J K^{-1} mol^{-1}	$\pi^{s,LFP}_{t=0}$ kJ mol^{-1}	$\pi^{s,LFP}_{t=\infty}$ kJ mol^{-1}
Yamada et al.[f) 18]	34 ± 2	Li_xFePO_4	0.003	1 M $LiPF_6$ 1:1 EC:DMC	12.8	30 ± 2	115 ± 7
			0.05		4.9	32 ± 2	117 ± 7
			0.15		−1.1	34 ± 2	119 ± 7
			0.45		−3.5	35 ± 2	120 ± 7
			0.60		−4.1	35 ± 2	120 ± 7
			0.80		−4.9	35 ± 2	120 ± 7
			0.90		−5.7	35 ± 2	120 ± 7
			1		−11.3	37 ± 2	122 ± 7
Viswanathan et al. [15]	34 ± 2 [18]	Li_xFePO_4	0	1 M $LiPF_6$ in 1:1 EC:DMC	7 ± 7	32 ± 5	117 ± 7
			0.10		1 ± 2	33 ± 2	118 ± 7
			0.20		−1.4 ± 0.4	34 ± 2	119 ± 7
			0.35		−2.5 ± 0.1	34 ± 2	119 ± 7
			0.50		−3.1 ± 0.2	35 ± 2	120 ± 7
			0.65		−3.9 ± 0.6	35 ± 2	120 ± 7
			0.80		−4.4 ± 0.6	35 ± 2	120 ± 7
			0.95		−6.1 ± 1.4	35 ± 2	120 ± 7
			1		−11.3 ± 1.1	37 ± 2	122 ± 7
Jalkanen et al.[g) 33]	34 ± 2 [18]	Li_xFePO_4	0	1 M $LiPF_6$ in EC:EMC:DMC	−2.4	34 ± 2	
			0.1		−3.8	35 ± 2	
			0.25		−4.7	35 ± 2	
			0.5		−4.1	35 ± 2	—
			0.75		−4.2	35 ± 2	
			1		−6.8	36 ± 2	

(e) $LiMn_2O_4$ (LMO) electrodes.

Authors [References]	$\pi^{s,Li}_{t=0}$ kJ mol^{-1} [References]	Electrode	x	Electrolyte	ΔS J K^{-1} mol^{-1}	$\pi^{s,LMO}_{t=0}$ kJ mol^{-1}	$\pi^{s,LMO}_{t=\infty}$ kJ mol^{-1}
Thomas et al.[h) 34]	34 ± 2 [18]	$Li_xMn_2O_4$	0.17	1 M $LiPF_6$ 1:1 EC:DMC	9 ± 5	31 ± 4	116 ± 7
			0.19 ± 0.01		23 ± 1	27 ± 2	112 ± 7
			0.30		14 ± 1	30 ± 2	115 ± 7
			0.42 ± 0.01		9 ± 5	31 ± 4	116 ± 7
			0.47		−10 ± 2	37 ± 2	122 ± 7
			0.52 ± 0.01		−30 ± 1	42 ± 2	127 ± 7

			0.60 ± 0.01		0.0 ± 0.3	34 ± 2	119 ± 7
			0.77 ± 0.01		−2 ± 3	34 ± 2	119 ± 7
			0.96		−21	40 ± 2	125 ± 7
			1		−29	42 ± 2	127 ± 7
			0.1		23	22 ± 1	—
			0.2		5	27 ± 1	—
			0.3		−1	29 ± 1	—
Kashiwagi et al.[69]	29 ± 1 [22]	$Li_xMn_2O_4$	0.45	1 M $LiClO_4$ EC:DEC	−14	33 ± 1	—
			0.55		12	25 ± 1	—
			0.65		18	23 ± 1	—
			0.75		−17	34 ± 1	—
			0.9		−32	38 ± 1	—

(f) $LiTiS_2$ (LTS) electrodes

Authors [References]	$\pi_{t=0}^{s,Li}$* kJ mol^{-1} [References]	Electrode	x	Electrolyte	ΔS J K^{-1} mol^{-1}	$\pi_{t=0}^{s,LTS}$ kJ mol^{-1}
			0.13		−9.3	32 ± 1
Honders et al. et al.[48]	29 ± 1	$Li_xTi_{1.03}$ S_2	0.61	1 M $LiClO_4$ in PC	−15.1	33 ± 1
			0.97		−28.1	37 ± 1
Wittingham[45] et al.	36 ± 2[21]	Li_xTiS_2	0.6	$LiPF_6$ in PC	−17	41 ± 2
		Li_xTiS_2	1		−37	47 ± 2
			0.04 ± 0.01		12.9 ± 0.6	32 ± 2
			0.14 ± 0.01		0.0 ± 0.6	36 ± 2
			0.18 ± 0.02		3.9 ± 0.5	34 ± 2
Dahn et al.	36 ± 2[21]	Li_xTiS_2	0.29	1 M $LiAsF_6$ in PC	6.1 ± 0.3	34 ± 2
			0.47		−10.4 ± 0.4	39 ± 2
			0.60 ± 0.02		−13 ± 1	40 ± 2
			0.83 ± 0.03		−17 ± 1	41 ± 2
			0.93 ± 0.01		−26 ± 2	43 ± 2

a) It was stated that the electrolyte used was molar $LiClO_4$ in polyethylene carbonate. We assume here that the authors meant instead 1 M $LiClO_4$ in PC. b) Error assumed given to one standard deviation in original work. c) Error assumed given to one standard deviation. d) x values estimated from SoC or *emf* data. e) x values estimated from SoC data. f) Values obtained from Viswanathan et al.[15] g) x values estimated from SoC or *emf* data. h) Entropy data for several cells was given, but not with identical x-values. The deviation in the entropy data for the different cells was used to estimate uncertainties. For some x, only one data point was available. As such, no uncertainty could be estimated and both the entropy and Peltier heat appear to have an artificially low uncertainty.

literature. Maeda et al., for instance, measured a cooling of graphite during de-intercalation,[64] which would mean a positive Peltier heat for the anode reaction. This observation was also made by Heubner et al. over a broad range of SoC.[17] They also reported that LCO cools during deintercalation and heats during intercalation, i.e. when it acts as an anode and cathode respectively.[17,52]

We conclude that there has been some confusion in the literature over the sign of the Peltier heat of lithium-reversible electrodes, but that there is consensus for the positive value, as listed in Tables Ia–Ib. A direct measurement of the electrode Peltier heat will confirm whether the electrode surface heats or cools during charge/discharge. The indirect determination of the Peltier heat, via a measurement of the Seebeck coefficient, provides a more accurate result,[65,66] as the direct method will always be hampered by thermal leakage.

The tables present Peltier heats that all have been computed from measured Seebeck coefficients. They are reported here using the sign convention explained above (see 19), when they perform as anodes. The same electrode, acting as a cathode, will have a Peltier heat of opposite sign as when it acts as an anode.

According to theory and Table Ib, the Peltier heat depends on the lithium salt in the electrolyte, but more on the degree of lithiation in the electrode, see also Figs. 6 and 7. The properties listed in the last column of the Tables Ib vary from the low value, 16 kJ mol^{-1}, for an initial state Peltier heat with (almost) zero lithium content, to the high value, 122 kJ mol^{-1} near 100 % SoC for the stationary state Peltier heat. This underlines the importance of doing measurements with varying SoC and until a stationary state has been reached.

Initial and stationary state reports on the Seebeck coefficient.— To the best of our knowledge, Richter et al.[24] were first to report stationary state Seebeck coefficients, cf. Table Ib bottom. The electrodes were of LCO and the electrolyte was 1 M $LiPF_6$ in EC:DEC in a preliminary report.[24] In a follow-up, we measured initial and stationary state values for electrodes of LFP and electrolyte of 1 M $LiPF_6$ in EC:DEC.[16] A significant difference between the initial and stationary state values was found, indicating that the Soret effect is substantial. In both measurements, the Seebeck coefficient was negative, giving a positive Peltier heat. The initial state Peltier heat of this case [16] has some support from results computed for $x = 1$ in Table IId, for an electrolyte of 1 M $LiPF_6$ in EC:DMC.

The difference between the initial and stationary state values of the Seebeck coefficient enabled us to estimate the sum $\sum_i t_i q_i^*$ in Eq. 17 for a 1 M $LiPF_6$ in a 1:1 w% EC:DEC solution. For this electrolyte, the sum amounted to 85 ± 7 kJ mol^{-1}. It appears important to do more experiments for stationary state conditions.

Summary so far.—It seems to be commonly accepted today that the LIB electrode|electrolyte interface will cool when acting as an anode, or heat when acting as a cathode. The literature contains confusion on the sign issue, so care must be taken to specify choice of convention. We shall use the sign convention that assigns the given Peltier heat to the lithium electrode when it acts as an anode.

There is nevertheless reasonable consensus in the data found on the value of the initial state Peltier heat of the electrode of pure

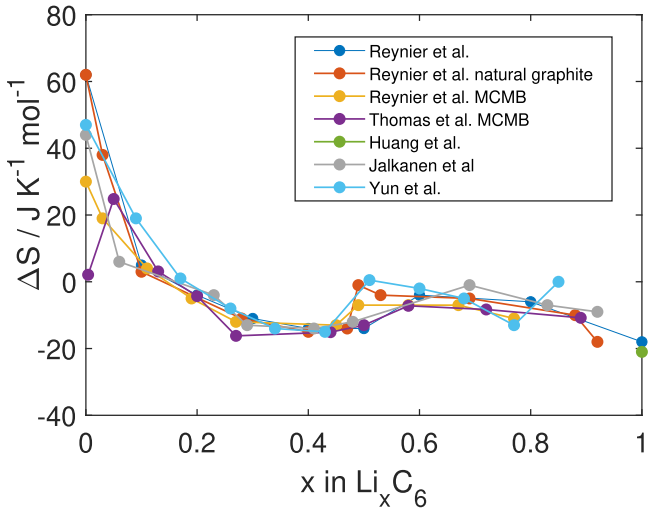

Figure 5. Half-cell entropy data for graphite, obtained from Reynier et al.,[36,37] Thomas et al.,[35] Huang et al.,[18] Jalkanen et al.[33] and Yun et al.[40] The values are also tabulated in Table IIb. The variation with degree of intercalation x is shown.

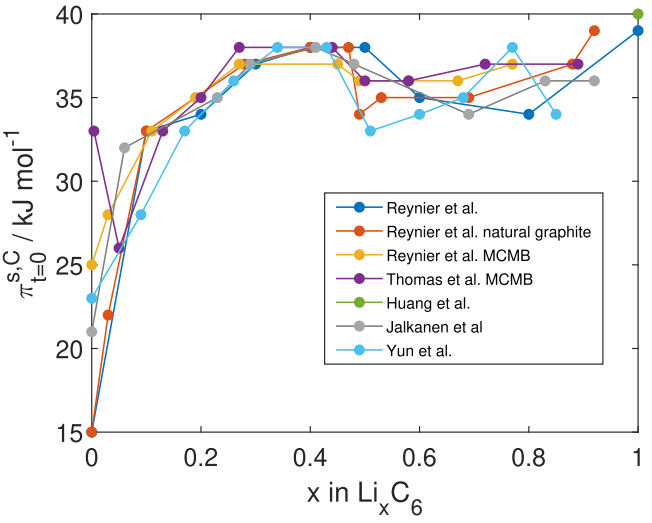

Figure 6. Initial state Peltier heats calculated for the graphite electrode at 298 K, using entropy data from Reynier et al.,[36,37] Thomas et al.,[35] Huang et al.,[18] Jalkanen et al.[33] and Yun et al.[40] Values were calculated from the initial state Peltier heats of Li metal given in Table Ia and half-cell entropy data from Table IIb. The variation with degree of intercalation x is shown.

lithium metal. It varies between 28 and 36 kJ mol^{-1} depending mostly on the lithium salt in the electrolyte. A larger variation is seen in the initial Peltier heat when lithium is intercalated in the electrode, from 16 to 20 kJ mol^{-1}. Also here, the data in the literature support one another.

Peltier Heats Computed from Half-cell Entropy Measurements

The Peltier heat of, say, the cathode can be determined from Eq. 4 for any electrode material at any state of charge. We need only to know the cell entropy and the Peltier heat of the other electrode, the anode. The electrolyte composition in the cells that we combined must be the same, however. The Peltier heat of the cathode is then:

$$\pi_t^{s,c} = \pi_t^{s,\mathrm{Li}} - T\Delta S \qquad [25]$$

where ΔS refers to cell discharge, and $\pi_t^{s,\mathrm{Li}}$ is the Peltier heat of the lithium anode at any state t. Equation 25 applies to stationary as well as initial states. The initial state Peltier heat of the Li metal electrode does not vary much with type of electrolyte, as was pointed out in connection with Tables Ia–Ib. The variation in the Peltier heat of the cathode, will therefore follow the variation in ΔS, with state of charge or temperature.

There are few reports on Peltier heats of LIB electrodes, but there are several reports on the cell entropy of LIBs, with electrodes at various lithiated states. In half-cells, the Li-metal electrode is usually the anode during discharge. The half-cell entropy measurements cited in Tables IIa–IIf represent an untapped source in this regard, as much data are available on these cells, thanks to the pioneering effort of Whittingham.[45] The cell measurements have often been done with well defined lithium content. We have taken advantage of this situation, and used reported cell entropy data of half-cells to estimate new Peltier heats of several electrodes at various states of charge, see Tables IIa–IIf. In these tables, we have listed reported values of ΔS obtained from half-cell measurements like with Fig. 2, and the Peltier heat for the Li-metal electrode from Table I, used in the calculation. The tabulated values provide a selection of data-points, chosen to show the trend which is typical for the half-cell entropy and the Peltier heat of each electrode. A more complete data-set may be obtained if needed from the entropy data in the original reference and the procedure described here to find Peltier heats.

The half-cell entropy change obtained with graphite-electrodes, and the corresponding initial state Peltier heat are presented in Figs. 5 and 6, respectively. The entropy change in Fig. 5 shows the now accepted variation from 30–60 J K^{-1} mol to −20 J K^{-1} mol through a local minimum at $x \approx 0.4$. The value can be positive as well as negative, depending on the composition. The corresponding Peltier heat in Fig. 6 is always positive, however. Peltier heats are tabulated as if the electrode in question were acting as an anode. A positive value means then that the electrode surface will cool, see Eq. 24.

The corresponding results for initial state Peltier heat-estimates for LCO are shown in Fig. 7. Data are accessible for a smaller range of x. The variations between the local minimum and maximum in the curves seem to be larger than for graphite, but all sets of data seem to vary in a similar way.

Some of the entropy data refer to electrolytes that do not match completely the electrolyte used for the Seebeck coefficient of Table Ia. In those cases, the Peltier heat of Li-metal with the most similar electrolyte was chosen for the calculation. As indicated by the data in Table Ia, the lithium salt is most decisive for the value. The accuracy of the resulting Peltier heats is hard to estimate, though the consistency in the Peltier heats of the Li-metal gives some

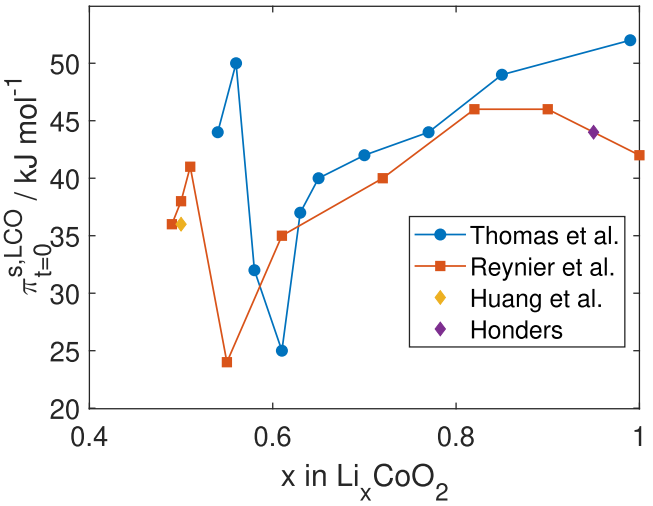

Figure 7. Initial state Peltier heats calculated for the $LiCoO_2$ electrode, computed from half-cell entropy data from Thomas et al.,[35] Reynier et al.,[58] Huang et al.[18] and Honders.[48] Values were calculated from the initial state Peltier heats of the Li metal shown in Table Ia and half cell entropy data in Table IIa. The variation with degree of intercalation x is shown.

assurance for the value used in the tables. It is listed with an uncertainty of two standard deviations in most cases.

As stated before, there is only one measurement on the difference between the initial and stationary state Seebeck coefficient; on the LIB electrolyte, 1 M $LiPF_6$ in EC:DEC.[16] Unfortunately this electrolyte is neither the most common for half-cell entropy measurements, nor has it been used in another Seebeck coefficient measurement. We are therefore at an impasse with regards to the stationary state Peltier heat. Nevertheless, it is interesting to use the stationary state data of 1 M $LiPF_6$ in EC:DEC to estimate stationary state Peltier heats for an electrolyte of 1 M $LiPF_6$ in EC:DMC. Doing this, we see that there is apparent agreement between the initial state estimate of Peltier heats for LFP given in Table Ib and the estimates of initial state Peltier heats in Table IId. This could indicate that the Dufour effects are similar.

The anode Peltier heats were first computed from their reciprocal Seebeck effects, for the method see Ref. 19. The initial state cathode Peltier heats seen in Tables IIa–IIf were next computed from the relation between the cell entropy change and the two Peltier heats in Eq. 4. The accuracy of the data presented hinges on the accuracy of the half-cell entropy -, and the Seebeck coefficient experiments. The uncertainty in the tabulated Peltier heats could be underestimated, as they reflect the uncertainties of two experiments. The uncertainty in the half-cell entropy measurements has frequently not been reported. Nevertheless, the data in Fig. 5 show good agreement, except maybe around 0% SoC. This is a good sign, especially when we know that the entropy data in Fig. 5 are taken from half-cell measurements where various graphitic materials are used, ranging from natural graphite to mesocarbon microbeads. Note, however, that entropy data of Saito and co-workers on a commercial LCO|hard carbon cell showed a different behavior than the commercial LCO| graphite cells.[41] This was most evident in the range 0%–50% SoC. In a graphite electrode, this range is where the most extreme changes happens in the cell entropy. Consequently, the Peltier heat is largest here. The data by Reynier et al. on carbons with a varying degree of graphitization suggest that the structure of the carbon anode has a large impact on both the entropy and Peltier heat.[59]

Discussion

Electrode Peltier heats: sign and magnitude variations.— Common to all Tables on the cell entropy change and the electrode Peltier heats, is that the cell entropy varies in sign, but the Peltier heat of the lithium electrode is always positive. This is so whether we are speaking of the lithium metal electrode, or of an electrode with lithium intercalation, see Tables IIa–IIf and Figs. 6–8. Also, most often the Peltier heats are much larger than the total reversible heat effect of the LIB. The consequence of this is that it is impossible to obtain the local heat effect at one electrode or to characterize the intercalation reaction as either endothermic or exothermic from half-cell entropy measurements only. Many investigators have attempted to do this,[9,44,57] while it cannot be done without prior knowledge of the Peltier heat of Li-metal. A similar argument was also presented by Huang et al.[18]

The Peltier heats in Tables I and II have not only a common sign, they also have rather similar magnitude. We can understand this by returning to the discussion of electrode heat effects above. Equation 19 can be used to explain the origin of the variation. The parameters sensitive to the composition are the transported entropy of the lithium ion, and the entropy of the intercalated lithium[16] sometimes called the excess entropy.[46] The transported entropy of lithium is large and positive.[16,24]

It is interesting to see that the electrodes with the largest reversible heat effect in the half-cell, such as graphite around $x = 0$, may have the smallest Peltier heat. This can be explained by Eq. 4. When the entropy change in a half-cell is positive, the Peltier heat of the corresponding electrode will be smaller, and vice versa. During discharge, the Peltier heat of graphite will be smaller than of Li, as long as the cell entropy change is positive. As previously mentioned, Kobayashi et al. and Lu et al. concluded from the half-cell entropy data that intercalation of lithium into graphite was exothermic, and for a small range of SoC endothermic.[9,57] The conclusion was drawn, despite the clear statement of Kobayashi et al. that a half-cell measurement contains an undetermined contribution from Li-metal. For their conclusion to be valid the Peltier heat of Li-metal must be 0, which we have seen is not the case. In fact, we see from Table IIb that the cooling effect can be explained by a lesser exothermic effect for graphite.

For some electrodes, the variation with x or SoC is small. This was true, in particular, for nickel-rich electrodes, such as $LiNi_{0.7}Co_{0.3}$ and NMC71515 (Table IIc) and LFP (Table IId), where Peltier heats similar to that of the Li- metal electrode were found. This agrees with half-cell entropy-data from commercial NMC electrodes,[70] and full-cell entropy-data from two LFP|graphite commercial cells.[42] Manganese-rich electrodes appear to have larger variations in Peltier heats than LFP and NMC electrodes have, but smaller than LCO, see Tables IIc and IIe. The findings were supported by the entropy measurements of Saito et al. on an LMO|graphite commercial cell.[56]

Also the stationary state Peltier heat is positive; the anode will therefore under all circumstances represent a heat sink. This is specific to the lithium electrode, and must be explained by the two large contributions to the Peltier heat in Eq. 19 the thermodynamic entropy of lithium and the transported entropy of lithium ion. The first property cannot be changed. The last will depend on electrolyte composition. The same applies to $t_i q_i^*$. The solvent would greatly affect the ion solvation shell and therefore t_i, q_i^* and $S^*_{Li^+}$.

Data available for thermal modelling.— Tables Ia and Ib present Peltier heats as computed from available information in the literature, using Eq. 17. The results are now available for thermal modelling of LiB initial states ($t = 0$). The reported values are reliable within the given accuracy.

In order to embark on transient modelling, we first note that the initial state Peltier heat may differ widely from the corresponding stationary state value, because the Dufour effect can be large. Equation 24 shows how the heat of transfer contributes to the change in the surface temperature during battery operation. To accurately model surface temperature, the stationary-state Peltier heat is needed.

In order to model cells with graphite electrodes care should be taken to use the proper degree of intercalation for the values listed in Table IIb. It is in the outset not possible to combine data from cells with different electrolytes. The transported entropy of lithium ion and the heats of transfer will vary. Clearly, more systematic measurements on a variety of compositions are needed to enable precise models (see also below).

Data missing in the literature.— As discussed above there is a gap in the knowledge on the importance of the Dufour/Soret effect for battery modelling. Measurements have made it clear that the Dufour effect can be significant.[16] This contradicts the common assumption in literature that the Dufour effect is negligible.[6] To neglect this effect, means to underestimate local heat effects.[11,61] Clearly there is a need for systematic investigations of the Dufour effect, *i.e.* the heat of transfer, q_i^*, in LIB electrolytes. Also needed is information on the transference coefficients t_i of organic solvent molecules. Such information is at present basically nonexistent. The lack of data on the Dufour effect significantly hampers thermal modelling of transient and stationary battery states.

The entropy change is clearly a function of SoC (or x), but also of the cell age.[40,71,72] Therefore, we expect that the Peltier heat is also a function of SoC and age. Also reported are small changes in entropy measurement results upon cycling.[73] If the Peltier heat is large compared to the cell entropy change, as measurements indicate,[16] a small change in the cell entropy change will not necessarily change the Peltier heat much. Nevertheless, results on Seebeck coefficients on pristine as well as aged electrodes could be helpful. As far as we know,

only pristine cells have been studied so far. The list of computed Peltier heats of individual electrodes in Table II is therefore still far from complete. It may be interesting to study also the contributions (the transported entropies, and the thermodynamic entropies) to the Peltier heats separately, for independent controls of their values.

Experiments are time-consuming, and at some point one may resort to computer simulations, which is possible to do for some of the terms in Eq. 4. There is a lack of data not only on the transported entropy of lithium ions, but also on heats of transfer and transference coefficients for a variety of electrolyte and electrolyte compositions and conditions.

The Peltier heats are temperature dependent, cf. Eq. 21. The Seebeck coefficients are therefore evaluated at the mean temperature of the cell. The Thompson coefficient is often small. Nevertheless, the relation (see Eqs. 4 and 21) $\Delta S = (\Delta\phi^{c}/\Delta T)_{j=0} - (\Delta\phi^{a}/\Delta T)_{j=0}$ indicates that the temperature-variation need be resolved. Measurements by Bazinski et al. on the graphite|LFP—full-cell indicated that ΔS varied much with temperature around 0% as well as around 100% SoC.[74] The group found ΔS at 0% SoC to be $-100\ \mathrm{J\ K^{-1}}$ mol at 45–50 ° C, while at $-10-(-15)$ ° C it was $-50\ \mathrm{J\ K^{-1}}$ mol. At 0% SoC, and with a computed Peltier heat of 37 kJ $\mathrm{mol^{-1}}$ for LFP at 298 K (see Eq. 21), we obtain at 323 K and 258 K a Peltier heat of 40.5 kJ $\mathrm{mol^{-1}}$ and 32.4 kJ $\mathrm{mol^{-1}}$. The Peltier heat of the graphite electrode interface can then be estimated to 8 and 19.5 kJ $\mathrm{mol^{-1}}$, respectively. Variations in the stationary state Peltier heat would be less significant when attention is paid to this effect. More data, both on the temperature dependence of the Seebeck coefficients and on the entropy change of half-cells would be needed in order to accurately determine the temperature dependence of Peltier heats.

Peltier heats of battery cells.—To translate half-cell entropy measurements into data for full-cell reversible heat effects, is not straight forward. This is because the degree of lithium intercalation in the electrode, x, or less precisely, its state of charge (SoC) may differ between the half- and full-cells for which data were obtained. In the combination of data, the same x need be used.

Particularly, for the anode material (the electrode where the anode reaction occurs during discharge), the half-cell SoC may not be the same as in the full-cell SoC. This is due to the procedure for making full-cells. Anodic material may be included in excess as a safety measure, to avoid lithium plating.[33] As lithium is lost from the electrode during the battery life-time,[75] the SoC-x ratio will change. For this reason we have chosen to report the entropy data in Tables IIa–IIf as a function of lithium content rather than as a function of SoC. The entropy change of the half-cell and the Peltier heat of the anode depend both on the entropy of intercalated lithium, $S_{\mathrm{Li(x)}}$. This entropy is a function of the lithium content, x. The dependence on SoC is indirect. The $x-$ dependence of $S_{\mathrm{Li(x)}}$ will not change throughout the battery life, though the range of $x-$ *values* might change. The same could not be said for SoC(x). The Peltier heats tabulated as function of x, are therefore most reliable.

Figure 8 compares values of initial Peltier heats for different electrode chemistries- Results are plotted against the relative lithium content in the cell. Some electrodes, such as lithium nickel manganese cobalt oxide (NMC) and lithium iron phosphate (LFP), have a very stable Peltier heat that varies little with x. To implement these data into a full-cell thermal model should be straightforward.

In full-cells with electrode materials, which show large variations in Peltier heats, the combination of results must take into account the composition dependence, as observed by several groups.[15,33] A case with a large composition-dependent Peltier heat, is the commercial cell of graphite|LFP. Half-cell and full-cell ΔS's were reported. In the full-cell, graphite was in excess, and the group found a graphite|LFP ratio of 1.35. This ratio was used to estimate the lithium content at 100% SoC, enabling us to assign the Peltier heats to SoC-values in the full-cell. The Peltier heats of the anode computed with data from Jalkanen et al.[33] are shown in Fig. 9 as a function of SoC. Results were taken from cells with different

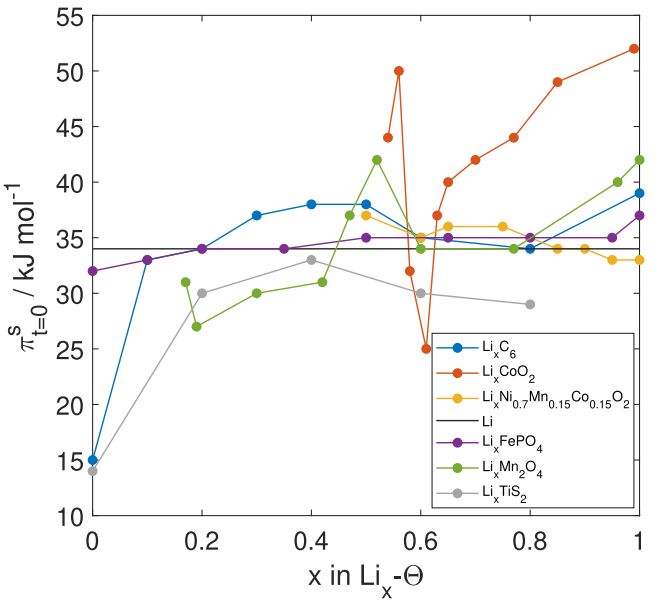

Figure 8. Initial state Peltier heats calculated at 298 K for the lithium intercalated electrodes as a function of degree of intercalation x in Li$_x$-Θ: Li$_x$C$_6$ (C),[37] Li$_x$CoO$_2$ (LCO), [35] Li$_x$Ni$_{0.7}$ Mn$_{0.15}$ Co$_{0.15}$ O$_2$ (NMC-71515),[40] lithium metal,[18] Li$_x$FePO$_4$ (LFP),[15] Li$_x$Mn$_2$O$_4$ (LMO)[34] and Li$_x$TiS$_2$ (LTS). The half-cell entropy data and the Peltier heat of the lithium metal used in the calculations, are shown in Tables IIa–IIf. The LTS values are computed from Seebeck coefficients, and the remaining values are estimated using half cell entropy data and the Peltier heat of Li-metal.

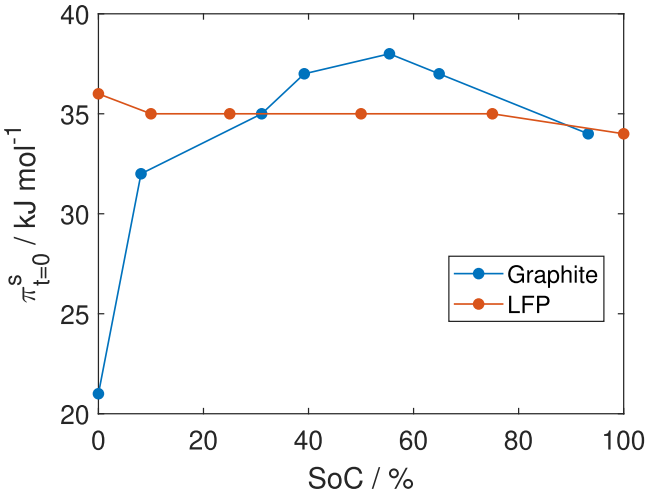

Figure 9. Full-cell initial state Peltier heats of the anode and cathode at 298 K in the commercial full-cell of graphite|LFP. Data were obtained from Jalkanen et al.[33]

electrolytes, but can nevertheless serve as an example of the interfacing procedure.

Blends of electrode materials are used to improve performance in commercial batteries.[76,77] How will this affect the Peltier heat? The Peltier heat of an electrode will in general mirror the half-cell entropy of the electrode, as seen above. If the half-cell entropy is a superposition of half-cell entropy curves of parent materials, as seen by Heubner et al.[78,79] and Huang et al.,[80] so will the Peltier heat. The outcome depends on the mass ratio and how well the electrode materials are blended. In short, on all factors that have an impact on the entropy.

Related battery cells are also emerging as industrial candidates. Examples include the sodium-ion[81] and lithium-sulfur (Li-S) batteries.[82] The difference between the Li-metal electrode Peltier

heat and Na-metal electrode Peltier heat comes from the standard partial molar entropy of Li and Na and the transported entropy of the lithium and sodium ions. The partial molar entropies are 28 and 51 J K^{-1} mol, respectively, and constant. The transported entropy of the electrons in the electrodes play a minor role. The transported entropy of the ions are harder to predict. The entropies of disodium polysulphides are large,[83] around 400 J K^{-1} mol. In aqueous systems large differences in the transported entropy has been found.[20] It is also likely that the transference coefficients differ from electrolyte to electrolyte, meaning that the Soret/Dufour effect will also vary. Electrolyte entropies depend normally strongly on complex formations, as evidenced by the high Seebeck coefficient of some organic electrolytes.[84] The entropy of intercalated Na-ions in the host-electrodes will also vary largely with composition. Speculations like these are not enough to answer fully on the importance of the reversible heat effects. More systematic measurements need to be done. For example, the Li-S battery will probably give a different Peltier heat for the Li-metal electrode than the values given in Table Ia, because the two batteries use different electrolytes (see Eq. 19). Quantitative model results calls for measured Peltier heats, however. The data presented in this article are therefore not directly applicable to new systems, but the present analysis indicate strongly that there are further needs for experimental works. Fortunately, the procedure used to obtain Peltier heats, from one Seebeck coefficient and cell entropy data, will be the same.

Summary and Outlook

We have seen in this review that the most important local reversible heat effect in lithium-ion batteries is the Peltier effect of the single electrode surface. From knowledge of the cell entropy and one electrode Peltier heat, the Peltier heat of the other electrode can be determined.

Earlier measurements of Seebeck coefficients of Li-metal thermoelectric cells and half-cell entropy data have here been exploited to give estimates of Peltier heats of various compositions and degrees of lithiation, for anodic reactions. The estimates have good reliability for the initial state Peltier heat, especially for the Li-electrode. There is a lack of data on the Dufour effect in LIB, which is needed to model the stationary state Peltier heat. This state is most relevant for thermal modelling of LIBs.

We have shown, using non-equilibrium thermodynamic theory, that electrodes previously associated with large reversible heat effects, may instead have small local heat effects. The importance of measuring the Peltier heat of one electrode, in addition to total reversible heat effect, has been pointed out, and exploited to obtain new Peltier heats.

For the lithium metal electrode functioning as an anode we propose as reference value of the initial Peltier heat, 34 ± 2 kJ mol^{-1} for an electrolyte with 1M $LiClO_4$, while the value is 29 ± 2 kJ mol^{-1} when the electrolyte contains 1 M $LiPF_6$. The values are not so sensitive to the organic solvent. The same is true for the Peltier heat of electrodes with lithium intercalation. This value can rise to $\approx$140 kJ mol^{-1} for the stationary state Peltier heat when the electrode performs as an anode. This is a large reversible heating effect, much larger than expected from the full cell entropy change itself. A systematic effort to find the Seebeck coefficient and half-cell entropy for more materials, aged or pristine, at initial and stationary state, will be useful. There is a need for more knowledge, in particular on Dufour effects, derived for instance from Seebeck coefficients at stationary and initial states. Better knowledge of the material's thermo-electric properties would, for instance, prevent battery models from possibly underestimating the interface temperatures.

Acronyms.

LIB	Lithium-ion battery
SoC	State-of-charge
OCV	Open circuit potential, *emf*
EC	Ethylene carbonate
DMC	Dimethyl carbonate
DEC	Diethyl carbonate
PC	Propylene carbonate
C	Lithiated graphite (LiC_6)
MCMB	Mesocarbon microbeads
LCO	Lithium cobalt oxide ($LiCoO_2$)
LFP	Lithium iron phosphate ($LiFePO_4$)
NMC	Lithium nickel manganese cobalt oxide ($LiNi_xMn_yCo_zO_2$)
LMO	Lithium manganese oxide ($LiMn_2O_4$)
NC	Lithium nickel cobalt oxide ($LiNi_xCo_zO_2$)
MC	Lithium manganese cobalt oxide ($LiMn_yCo_zO_2$)
LTS	Litcide $LiTiS_2$

Symbol lists.

(a) Greek letters

Symbol	Dimension	Explanation
Δ	—	Change in a quantity or variable
Θ	—	Electrode host structure
λ		Thermal conductivity at stationary state
μ_i	J mol^{-1}	Chemical potential of component i
π^{k}	J mol^{-1}	Peltier coefficient
$\pi_t^{\mathrm{s,i}}$	J mol^{-1}	Peltier heat of surface s with adjoining bulk phase i computed from Seebeck coefficient measured at time t
ρ^{s}	kg m^{-2}	Excess density of surface
ϕ	V	Electric potential

(b) Roman letters

Symbol	Dimension	Explanation
a_{ij}	J mol^{-1}	Coefficient for describing chemical potential gradients evaluated at constant temperature from linear combination of concentration gradients
c_i	mol m^{-3}	Concentration of component i
C^{s}	J K^{-1} kg^{-1}	Specific heat capacity of surface
$D_{i,T}$	m^2 s^{-1} K^{-1}	Thermal diffusion coefficient of component i
D_{ij}	m^2 s^{-1}	Interdiffusion coefficient

(Continued).

(b) Roman letters

F	C mol^{-1}	Faraday's constant
$\Delta_n G^s$	J mol^{-1}	Reaction Gibbs energy of neutral surface components
H_i	J mol^{-1}	Partial molar enthalpy of component i
j	A m^{-2}	Current density
J_i	mol m^{-2} s^{-1}	Molar flux of component i
J_q'	J m^{-2} s^{-1}	Measurable heat flux
n	—	Number of electrons involved in electrode reactions
r	m^{-1}	Ohmic resistivity
q	J m^2 s^{-1}	Reversible heat generation
q_i^*	J mol^{-1}	Heat of transfer of component i
S	J K^{-1} mol^{-1}	Entropy
S_i	J K^{-1} mol^{-1}	Partial molar entropy of component i
S_i^*	J K^{-1} mol^{-1}	Transported entropy of component i
t_i	—	Transference coefficient of component i
t	s	Time
T	K	Temperature

(c) Super- and subscripts

tot	Total
k	Phase k
s,i	Surface property with adjoining bulk phase i
i	Phase i
o	Phase o
l	Left-hand side
r	Right-hand side
s	Surface property
e	Electrolyte
a	Anode
c	Cathode
$t = 0$	Initial state
$t = \infty$	Stationary state

Acknowledgments

The authors A.F.G and S.K are grateful to the Centre of Excellence Funding Scheme from the Norwegian Research Council, PoreLab project no. 262 644.

ORCID

Astrid F. Gunnarshaug https://orcid.org/0000-0002-8452-4543
Signe Kjelstrup https://orcid.org/0000-0003-1235-5709

References

1. R. Marom, S. F. Amalraj, N. Leifer, D. Jacob, and D. Aurbach, "A review of advanced and practical lithium battery materials." *Journal of Materials Chemistry*, **21**, 9938 (2011).
2. J. B. Goodenough and Y. Kim, "Challenges for rechargeable Li batteries." *Chemistry of materials*, **22**, 587 (2010).
3. H. Liu, Z. Wei, W. He, and J. Zhao, "Thermal issues about Li-ion batteries and recent progress in battery thermal management systems: A review." *Energy conversion and management*, **150**, 304 (2017).
4. T. Estrup, E. Gagatsi, and A. Halatsis, "Exploring the potentials of electrical waterborne transport in europe: The e-ferry concept." *Transportation Research Procedia, Transport Research Arena TRA2016*, **14**, 1571 (2016).
5. L. Rao and J. Newman, "Heat-generation rate and general energy balance for insertion battery systems." *J. Electrochem. Soc.*, **144**, 2697 (1997).
6. W. B. Gu and C. Y. Wang, "Thermal-electrochemical modeling of battery systems." *J. Electrochem. Soc.*, **147**, 2910 (2000).
7. E. V. Thomas, I. Bloom, J. P. Christophersen, and V. S. Battaglia, "Statistical methodology for predicting the life of lithium-ion cells via accelerated degradation testing." *Journal of Power Sources*, **184**, 312 (2008).
8. F. Richter, P. J. S. Vie, S. Kjelstrup, and O. S. Burheim, "Measurements of ageing and thermal conductivity in a secondary NMC-hard carbonLi-ion battery and the impact on internal temperature profiles." *Electrochimica Acta*, **250**, 228 (2017).
9. Y. Kobayashi, H. Miyashiro, K. Kumai, K. Takei, T. Iwahori, and I. Uchida, "Precise electrochemical calorimetry of $LiCoO_2$/graphite lithium-ion cell." *J. Electrochem. Soc.*, **149**, A978 (2002).
10. C.-H. Doh, Y.-C. Ha, and S. Eom, "Entropy measurement of a large format lithium ion battery and its application to calculate heat generation." *Electrochimica Acta*, **309**, 382 (2019).
11. L. Spitthoff, A. F. Gunnarshaug, D. Bedeaux, O. Burheim, and S. Kjelstrup, "Peltier effects in lithium-ion battery modeling." *The Journal of Chemical Physics*, **154**, 114705 (2021).
12. K. Smith and C.-Y. Wang, "Power and thermal characterization of a lithium-ion battery pack for hybrid-electric vehicles." *Journal of Power Sources*, **160**, 662 (2006).
13. B. Wu, V. Yufit, M. Marinescu, G. J. Offer, R. F. Martinez-Botas, and N. P. Brandon, "Coupled thermal-electrochemical modelling of uneven heat generation in lithium-ion battery packs." *Journal of Power Sources*, **243**, 544 (2013).
14. V. Srinivasan and C. Y. Wang, "Analysis of electrochemical and thermal behavior of li-ion cells." *J. Electrochem. Soc.*, **150**, A98 (2003).
15. V. V. Viswanathan, D. Choi, D. Wang, W. Xu, S. Towne, R. E. Williford, J.-G. Zhang, J. Liu, and Z. Yang, "Effect of Entropy Change of Lithium Intercalation in Cathodes and Anodes on Li-ion Battery Thermal Management." *Journal of Power Sources*, **195**, 3720 (2010).
16. A. F. Gunnarshaug, S. Kjelstrup, D. Bedeaux, F. Richter, and O. S. Burheim, "The reversible heat effects at lithium iron phosphate-and graphite electrodes." *Electrochimica Acta*, **337**, 135567 (2020).
17. C. Heubner, M. Schneider, C. Lämmel, and A. Michaelis, "Local heat generation in a single stack lithium ion battery cell." *Electrochimica Acta*, **186**, 404 (2015).
18. Q. Huang, M. Yan, and Z. Jiang, "Thermal study on single electrodes in lithium-ion battery." *Journal of Power Sources*, **156**, 541 (2006).
19. K. S. Førland, T. Førland, and S. K. Ratkje, *Irreversible thermodynamics: theory and applications* (John Wiley & Sons Incorporated, Chichester) (1988).
20. S. Kjelstrup and D. Bedeaux, *Non-equilibrium thermodynamics of heterogeneous systems* (World Scientific, Singapore) 2 (2020).
21. N. S. Hudak and G. G. Amatucci, "Energy harvesting and storage with lithium-ion thermogalvanic cells." *J. Electrochem. Soc.*, **158**, A572 (2011).
22. J. J. Black, J. B. Harper, and L. Aldous, "Temperature effect upon the thermo-electrochemical potential generated between lithium metal and lithium ion

intercalation electrodes in symmetric and asymmetric battery arrangements." *Electrochemistry Communications*, **86**, 153 (2018).
23. Y. V. Kuzminskii, V. A. Zasukha, and G. Y. Kuzminskaya, "Thermoelectric effects in electrochemical systems. nonconventional thermogalvanic cells." *Journal of Power Sources*, **52**, 231 (1994).
24. F. Richter, A. F. Gunnarshaug, O. S. Burheim, P. J. S. Vie, and S. Kjelstrup, "Single Electrode Entropy Change for $LiCoO_2$ Electrodes." *ECS Transactions*, **80**, 219 (2017).
25. Q. Xu, S. Kjelstrup, and B. Hafskjold, "Estimation of single electrode heats." *Electrochimica Acta*, **43**, 2597 (1998).
26. J. N. Agar and J. C. R. Turner, "Thermal diffusion in solutions of electrolytes." *Proceedings of the Royal Society of London. Series A, Mathematical and Physical Sciences***255**, 307 (1960).
27. J. N. Agar and W. G. Breck, "Thermal Diffusion in Non-Isothermal Cells: Part 1.-Theoretical Relations and Experiments on Solutions of Thallous Salts." *Transactions of the Faraday Society*, **53**, 67 (1957).
28. T. I. Quickenden and Y. Mua, "A review of power generation in aqueous thermogalvanic cells." *J. Electrochem. Soc.*, **142**, 3985 (1995).
29. A. Gunawan, C.-H. Lin, D. A. Buttry, V. Mujica, R. A. Taylor, R. S. Prasher, and P. E. Phelan, "Liquid thermoelectrics: Review of recent and limited new data of thermogalvanic cell experiments." *Nanoscale and Microscale Thermophysical Engineering*, **17**, 304 (2013).
30. R. H. Gerke, "Temperature coefficient of electromotive force of galvanic cells and the entropy of reactions." *J. Am. Chem. Soc.*, **44**, 1684 (1922).
31. J. M. Sherfey and A. Brenner, "Electrochemical calorimetry." *J. Electrochem. Soc.*, **105**, 665 (1958).
32. K. Onda, H. Kameyama, T. Hanamoto, and K. Ito, "Experimental study on heat generation behavior of small lithium-ion secondary batteries." *J. Electrochem. Soc.*, **150**, A285 (2003).
33. K. Jalkanen, T. Aho, and K. Vuorilehto, "Entropy change effects on the thermal behavior of a $LiFePO_4$/graphite lithium-ion cell at different states of charge." *Journal of Power Sources*, **243**, 354 (2013).
34. K. E. Thomas, C. Bogatu, and J. Newman, "Measurement of the entropy of reaction as a function of state of charge in doped and undoped lithium manganese oxide." *J. Electrochem. Soc.*, **148**, A570 (2001).
35. K. E. Thomas and J. Newman, "Heats of mixing and of entropy in porous insertion electrodes. Selected papers presented at the 11th International Meeting on Lithium Batteries." *Journal of Power Sources*, **119-121**, 844 (2003).
36. Y. Reynier, R. Yazami, and B. Fultz, "Thermodynamics of lithium intercalation into graphites and disordered carbons." *J. Electrochem. Soc.*, **151**, A422 (2004).
37. Y. Reynier, R. Yazami, and B. Fultz, "The entropy and enthalpy of lithium intercalation into graphite." *Journal of Power Sources*, **119**, 850 (2003).
38. Y. Reynier, R. Yazami, and B. Fultz, "Thermodynamics of lithium intercalation into graphites and disordered carbons." *J. Electrochem. Soc.*, **151**, A422 (2004).
39. X.-F. Zhang, Y. Zhao, Y. Patel, T. Zhang, W.-M. Liu, M. Chen, G. J. Offer, and Y. Yan, "Potentiometric measurement of entropy change for lithium batteries." *Phys. Chem. Chem. Phys.*, **19**, 9833 (2017).
40. F. Yun, W. Jin, L. Tang, W. Li, J. Pang, and S. Lu, "Analysis of capacity fade from entropic heat coefficient of $Li[Ni_xCo_yMn_z]O_2$/graphite lithium ion battery." *J. Electrochem. Soc.*, **163**, A639 (2016).
41. K. Takano, Y. Saito, K. Kanari, K. Nozaki, K. Kato, A. Negishi, and T. Kato, "Entropy change in lithium ion cells on charge and discharge." *Journal of Applied Electrochemistry*, **32**, 251 (2002).
42. J. P. Schmidt, A. Weber, and E. Ivers-Tiffée, "A novel and precise measuring method for the entropy of lithium-ion cells: ?s via electrothermal impedance spectroscopy." *Electrochimica Acta*, **137**, 311 (2014).
43. S. A. Hallaj, J. Prakash, and J. R. Selman, "Characterization of commercial Li-ion batteries using electrochemical-calorimetric measurements." *Journal of Power Sources*, **87**, 186 (2000).
44. S. A. Hallaj, R. Venkatachalapathy, J. Prakash, and J. R. Selman, "Entropy changes due to structural transformation in the graphite anode and phase change of the $LiCoO_2$ cathode." *J. Electrochem. Soc.*, **147**, 2432 (2000).
45. M. S. Whittingham, "Chemistry of intercalation compounds: Metal guests in chalcogenide hosts." *Progress in Solid State Chemistry*, **12**, 41 (1978).
46. A. H. Thompson, "Thermodynamics of Li intercalation batteries: Entropy measurements on Li_xTiS_2." *Physica B+C*, **105**, 461 (1981).
47. J. R. Dahn and R. R. Haering, "Entropy measurements on Li_xTiS_2." *Can. J. Phys.*, **61**, 1093 (1983).
48. A. Honders, J. M. der Kinderen, A. H. van Heeren, J. H. W. de Wit, and G. H. J. Broers, "The thermodynamic and thermoelectric properties of Li_xTiS_2 and Li_xCoO_2." *Solid State Ionics*, **14**, 205 (1984).
49. J. P. Pereira-Ramos, R. Messina, C. Piolet, and J. Devynck, "A thermodynamic study of electrochemical lithium insertion into vanadium pentoxide." *Electrochimica Acta*, **33**, 1003 (1988).
50. S. Bach, J. P. Pereira-Ramos, N. Baffier, and R. Messina, "Thermodynamic data of electrochemical lithium intercalation in $Li_xMn_2O_4$." *Electrochimica Acta*, **37**, 1301 (1992).
51. A. V. Popov, Y. G. Metlin, and Y. D. Tretyakov, "Thermodynamics of ordering in β-$Li_xV_2O_5$ lithium-vanadium oxide bronzes." *J. Solid State Chem.*, **32**, 343 (1980).
52. J.-S. Hong, H. Maleki, S. A. Hallaj, L. Redey, and J. R. Selman, "Electrochemical-calorimetric studies of lithium-ion cells." *J. Electrochem. Soc.*, **145**, 1489 (1998).
53. D. Bernardi, E. Pawlikowski, and J. Newman, "A general energy balance for battery systems. Selected papers presented at the 11th International Meeting on Lithium Batteries." *J. Electrochem. Soc.*, **132**, 5 (1985).
54. J. Newman, K. E. Thomas, H. Hafezi, and D. R. Wheeler, "Modeling of lithium-ion batteries." *Journal of Power Sources*, **119–121**, 838 (2003).
55. N. A. Godshall and J. R. Driscoll, "Determination of the thermoneutral potential of li/SOCl2 cells." *J. Electrochem. Soc.*, **131**, 2221 (1984).
56. Y. Saito, K. Kanari, and K. Takano, "Thermal studies of a lithium-ion battery. Proceedings of the Eighth International Meeting on Lithium Batteries." *Journal of Power Sources*, **68**, 451 (1997).
57. H. Yang and W. Lu, "and Jai Prakash. Determination of the reversible and irreversible heats of $LiNi_{0.8}Co_{0.2}O_2$/mesocarbon microbead Li-ion cell reactions using isothermal microcalorimetery." *Electrochimica Acta*, **51**, 1322 (2006).
58. Y. Reynier, J. Graetz, T. Swan-Wood, P. Rez, R. Yazami, and B. Fultz, "Entropy of Li intercalation in Li_xCoO_2." *Physical Review B*, **70**, 174304 (2004).
59. Y. Reynier, R. Yazami, B. Fultz, and I. Barsukov, "Evolution of lithiation thermodynamics with the graphitization of carbons." *Journal of Power Sources*, **165**, 552 (2007), IBAHBC 2006.
60. K. Kai, Y. Kobayashi, H. Miyashiro, G. Oyama, S. Nishimura, M. Okubo, and A. Yamada, "Particle-size effects on the entropy behavior of a Li_xFePo_4 electrode." *ChemPhysChem*, **15**, 2156 (2014).
61. J. Newman, "Thermoelectric effects in electrochemical systems." *Industrial & engineering chemistry research*, **34**, 3208 (1995).
62. A. F. Gunnarshaug, S. Kjelstrup, and D. Bedeaux, "The heat of transfer and the peltier coefficient of electrolytes." *Chemical Physics Letters: X*, **5**, 100040 (2020).
63. M. J. Schmid, K. R. Bickel, P. Novák, and R. Schuster, "Microcalorimetric measurements of the solvent contribution to the entropy changes upon electrochemical lithium bulk deposition." *Angew. Chem. Int. Ed.*, **52**, 13233 (2013).
64. Y. Maeda, "Thermal behavior on graphite due to electrochemical intercalation." *J. Electrochem. Soc.*, **137**, 3047 (1990).
65. H. J. V. Tyrrell, D. A. Taylor, and C. M. Williams, "The seebeck effect in a purely ionic system." *Nature*, **177**, 668 (1956).
66. J. N. Agar, *Thermogalvanic cells in advances in electrochemistry and electrochemical engineering*, ed. P. Delahay (Interscience, New York) (1963).
67. L. E. Downie, L. J. Krause, J. C. Burns, L. D. Jensen, V. L. Chevrier, and J. R. Dahn, "In situ detection of lithium plating on graphite electrodes by electrochemical calorimetry." *J. Electrochem. Soc.*, **160**, A588 (2013).
68. M. J. Schmid, *Wärmeeffekte bei der lithiumabscheidung und-interkalation-mikrokalorimetrische untersuchungen zur reaktionsentropie in lithium/graphit-halbzellen*, Institut für Physikalische Chemie, Karlsruher Institut für Technologie (KIT) (2014).
69. T. Kashiwagi, M. Nakayama, K. Watanabe, M. Wakihara, Y. Kobayashi, and H. Miyashiro, "Relationship between the electrochemical behavior and Li arrangement in $Li_xM_yMn_{2-y}O_4$ (M = Co, Cr) with spinel structure." *The Journal of Physical Chemistry B*, **110**, 4998 (2006).
70. R. E. Williford, V. V. Viswanathan, and J.-G. Zhang, "Effects of entropy changes in anodes and cathodes on the thermal behavior of lithium ion batteries." *Journal of Power Sources, Selected Papers presented at the 14th INTERNATIONAL MEETING ON LITHIUM BATTERIES (IMLB-2008)*, **189**, 101 (2009).
71. K. Maher and R. Yazami, "A study of lithium ion batteries cycle aging by thermodynamics techniques." *Journal of Power Sources*, **247**, 527 (2014).
72. J. Geder, R. Arunachala, S. Jairam, and A. Jossen, "Thermal behavior of aged lithium-ion batteries: calorimetric observations." *2015 IEEE Green Energy and Systems Conference (IGESC)*, 24 (2015).
73. N. S. Hudak, L. E. Davis, and G. Nagasubramanian, "Cycling-induced changes in the entropy profiles of lithium cobalt oxide electrodes." *J. Electrochem. Soc.*, **162**, A315 (2014).
74. S. J. Bazinski and X. Wang, "The influence of cell temperature on the entropic coefficient of a lithium iron phosphate (LFP) pouch cell." *J. Electrochem. Soc.*, **161**, A168 (2013).
75. J. B. Goodenough and K.-S. Park, "The li-ion rechargeable battery: a perspective." *J. Am. Chem. Soc.*, **135**, 1167 (2013).
76. C. Heubner, T. Liebmann, M. Schneider, and A. Michaelis, "Recent insights into the electrochemical behavior of blended lithium insertion cathodes: A review." *Electrochimica Acta*, **269**, 745 (2018).
77. S. B. Chikkannanavar, D. M. Bernardi, and L. Liu, "A review of blended cathode materials for use in li-ion batteries." *Journal of Power Sources*, **248**, 91 (2014).
78. C. Heubner, M. Schneider, and A. Michaelis, "Reversible heat generation rates of blended insertion electrodes." *Journal of Solid State Electrochemistry*, **21**, 2109 (2017).
79. T. Liebmann, C. Heubner, M. Schneider, and A. Michaelis, "Investigations on the reversible heat generation rates of blended li-insertion electrodes." *Journal of Solid State Electrochemistry*, **23**, 245 (2019).
80. J. Huang, Z. Li, B. Y. Liaw, Z. Wang, S. Song, N. Wu, and J. Zhang, "Entropy coefficient of a blended electrode in a lithium-ion cell." *J. Electrochem. Soc.*, **162**, A2367 (2015).
81. M. D. Slater, D. Kim, E. Lee, and C. S. Johnson, "Sodium-ion batteries." *Adv. Funct. Mater.*, **23**, 947 (2013).
82. S. S. Zhang, "Liquid electrolyte lithium/sulfur battery: Fundamental chemistry, problems, and solutions." *Journal of Power Sources*, **231**, 153 (2013).
83. V. S. Sharivker, S. K. Ratkje, and B. Cleaver, "Determination of the entropy of molten disodium polysulphides." *Electrochimica Acta*, **41**, 2381 (1996).
84. M. Bonetti, S. Nakamae, M. Roger, and P. Guenoun, "Huge seebeck coefficients in nonaqueous electrolytes." *The Journal of Chemical Physics*, **134**, 114513 (2011).